Riverine nutrient impact on global ocean nitrogen cycle feedbacks and marine primary production in an Earth System Model

Miriam Tivig[1,2], David P. Keller[1,3], and Andreas Oschlies[1]

[1]GEOMAR Helmholtz-Zentrum für Ozeanforschung Kiel, Wischhofstr. 1-3, D-24148 Kiel, Germany
[2]Deutscher Wetterdienst, Abteilung Klima und Umwelt, Michendorfer Chaussee 23, D-14473 Potsdam, Germany.
[3]Carbon to Sea Initiative

Correspondence: Miriam Tivig (mtivig@geomar.de)

Abstract.

   Riverine nutrient export is an important process in marine coastal biogeochemistry and also impacts global marine biology. The nitrogen cycle is a key player here. Internal feedbacks regulate not only nitrogen distribution, but also primary production and thereby oxygen concentrations. Phosphorus is another essential nutrient and interacts with the nitrogen cycle via different feedback mechanisms. After a previous study of the marine nitrogen cycle response to riverine nitrogen supply, we here include phosphorus from river export with different phosphorus burial scenarios and study the impact of phosphorus alone and in combination with nitrogen in a global 3-D ocean biogeochemistry model. Again, we analyse the effects on near coastal and open ocean biogeochemistry. We find that the addition of bio-available riverine phosphorus alone or together with nitrogen affects marine biology on millennial timescales more than riverine nitrogen alone. Biogeochemical feedbacks in the marine nitrogen cycle are strongly influenced by additional phosphorus. Where bio-available phosphorus is increased by river input, nitrogen concentration increases as well, except for regions with high denitrification rates. High phosphorus burial rates decrease biological production significantly. Globally, riverine phosphorus leads to elevated primary production rates in the coastal and open oceans.

Plain Language Summary

Coastal oceans are the most productive parts of the global ocean and, arguably, most sensitive to environmental change, but poorly resolved in most global models. In reality, rivers influence the coastal oceans, because they transport nutrients from land to the sea. This nutrient supply is often not included in global models, even though it may impact not only the coastal biology, but also the marine biology in regions farther away. We here include dissolved inorganic nitrogen and phosphorus from river export in a global ocean model and study the effects on the near coastal and the open ocean. We find that the addition of riverine phosphorus affects marine biology on millennial timescales more than riverine nitrogen alone. Where phosphorus is increased by river input, nitrogen concentrations increase as well, except for regions with high rates of bacterial consumption of nitrate (denitrification). High phosphorus burial rates on the other hand, decrease biological production significantly. Globally, riverine phosphorus leads to higher primary production rates in the coastal and open oceans.

1 Introduction

Nitrogen and phosphorus are both considered as limiting nutrients in the global ocean. 'Limiting' refers here to the concept of Liebig's law of growth rate determined by the availability of the most limiting substrate (Allaby, 2010). It states that growth is dictated not by total resources available, but by the scarcest resource (limiting factor). Nitrogen can be considered as the 'proximate limiting' and phosphorus as the 'ultimate limiting' nutrient, according to the definition by Tyrrell (1999). Changes in the availability of oceanic fixed-nitrogen (N) are known to have driven marine productivity changes, thereby regulating the strength of the biological carbon pump. By this, the availability of N also influences the carbon cycle in atmosphere and ocean (Falkowski, 1997). Phosphorus (P) is limiting marine productivity on geological and global scales and plays an important role in regulating oceanic oxygen inventories (Monteiro et al., 2012; Palastanga et al., 2011).

Oceanic fixed nitrogen concentrations are mainly controlled by the balance between nitrogen fixation and denitrification, but atmospheric deposition and riverine input also contribute to the global N budget (Somes et al., 2013; Deutsch et al., 2007; Gruber, 2004; Ruttenberg, 2003). Although several studies question the stability of the marine N inventory (Zehr and Capone, 2020; Codispoti et al., 2001; Gruber and Sarmiento, 1997; Codispoti, 1995), the pre-industrial global nitrogen cycle is often assumed to reflect a steady state (Deutsch et al., 2007; Altabet, 2006; Gruber, 2004; Tyrrell, 1999; Redfield et al., 1963).

This balance is assured by negative N-cycle feedbacks that stabilize marine N concentration: Where fixed N is sparse, diazotrophs can fix atmospheric N_2 instead of depending on dissolved inorganic nitrogen (DIN), such as ammonia or nitrate. But as the process of atmospheric N fixation is slower and requires more energy, mostly to keep oxygen away from the oxygen-sensitive enzyme nitrogenase, diazotrophs are rapidly outcompeted by other phytoplankton who do not have this energetic cost, if sufficient DIN is available. Growth of diazotrophs is also limited by the availability of phosphate, light and iron.

On the other hand, the global N budget is regulated by loss of fixed N, predominantly via denitrification. This process describes anaerobic respiration of organic matter via bacterial reduction of nitrate to N_2, and occurs in the water column as well as in sediments if the oxygen concentration is low (Gruber, 2004; Deutsch et al., 2001). Denitrification limits itself, as the consumption of nitrate leads to a reduction in the production of organic matter and hence to less oxygen consumption.

Generally the processes of N_2-fixation and denitrification take place in different regions of the world ocean. Still, feedbacks link these processes globally and are generally assumed to restore the balance in the global marine N budget. In some regions, however, N_2-fixation and denitrification occur in geographical proximity and may produce a "vicious cycle" with a runaway local loss of fixed N (Landolfi et al., 2013). Estimates of the mean residence time of fixed nitrogen in the global ocean amount to a few thousand years (Gruber, 2004). Due to the complexity of internal feedbacks and the dynamic role of nitrogen in the marine biological production it is difficult to assess, how sensitive the global N concentration is to perturbations of marine biogeochemistry.

In a previous study (Tivig et al., 2021), we used the Earth system climate model of intermediate complexity of the University of Victoria (UVic) version 2.9 (Eby et al., 2009; Weaver et al., 2001) to study N cycle feedbacks in the modelled ocean in

response to the addition of riverine dissolved inorganic nitrogen (Tivig et al., 2021). We found that, although in hot-spots near the river mouths marine primary production increased due to the additional N, globally biogeochemical feedbacks stabilized DIN concentrations and primary production, and could even lead to a local decline in DIN and productivity in proximity to low oxygen regions. In those idealized simulations, N was the only nutrient supplied via rivers.

With this, we confirmed an early study by Tyrrell (1999), who used a box model and found, that "an increase in the river delivery of nitrate has no long-term effect on productivity". But Tyrrell (1999) also concluded, that "an increase in the river delivery of phosphate, on the other hand, causes a sustained and proportionate increase in productivity". The interaction between fixed N and phosphorus (P) is of particular interest for marine primary production. The availability of P is one of the limiting factors for N_2 fixation (Wang et al., 2019; Landolfi et al., 2015).

In Tivig et al. (2021) we also found, that locally, marine productivity has been increased by riverine N supply. Riverine supply of P, is predicted to regulate total ocean productivity globally (Tyrrell, 1999). Nevertheless, locally, in coastal oceans and in regions with low oxygen concentrations, marine biogeochemistry can differ from global averages.

The total P inventory in the global ocean is mainly controlled by riverine input and burial at the seafloor (Wallmann, 2010; Ruttenberg, 2003; Baturin, 2003; Delaney, 1998). The residence time of P in the global ocean is approximately one order of magnitude longer than that of fixed N (Delaney, 1998). (Bio-)chemical weathering on continents represents the main source of riverine bio-available P (Filipelli, 2008; Föllmi, 1995). Changes in marine P are mostly a consequence of changes in terrestrial weathering and therefore have generally occurred on geological timescales.

Nevertheless, climate change and direct anthropogenic interventions in the P cycle have started to alter P fluxes during the last century. Due to the wide-spread use of fertilizers, to deforestation and sewage sources, the riverine load of phosphorus has increased globally (Seitzinger et al., 2010; Filipelli, 2008). In addition, river flows have also been dramatically altered by land use change and the damming of rivers (Cappellen and Maavara, 2016). In order to predict future changes in marine biogeochemistry, it is therefore relevant to understand, how P fluxes impact the marine N cycle, the N cycle feedbacks and marine productivity globally and regionally.

As global observations and measurements of ocean nutrients and fluxes are difficult and observations still relatively sparse, models are often used to investigate large-scale marine biogeochemistry over long time scales. However, only recently have there been more global modelling studies with riverine nutrient input. In one of the first studies, Giraud et al. (2008) analysed coastal fluxes of P, silicate, and dissolved iron in a global ocean model and found that including nutrients in the coastal ocean impacts biological activity locally but also in the open ocean. They also found, that excess nutrients in the coastal ocean can impact the open ocean biogeochemistry depending on which nutrient is advected from the coastal region. Nutrient availability and its consumption in the coastal domain control this advection. Additional P does affect coastal oceans especially if they are P-limited and if they are not limited by other nutrients like iron. In this case, Giraud et al. (2008) found that increased primary production in the coastal oceans can lead to a depletion of nutrients in the open ocean, reducing biological activity there. This "seesaw effect" was detected by Giraud et al. (2008) on local and global scale. If P is not consumed in the coastal oceans, it may be advected offshore, eventually increasing primary production there. N was not simulated explicitly in that study but coupled to P via Redfield ratio. The simulation performed by (Giraud et al., 2008) was only run for 10 years, hence not long

enough for N-cycle feedbacks to materialise.

In a more recent study (Lacroix et al., 2020) implemented estimated riverine nutrient loads of P, N, iron, carbon (C) and silica in a global ocean model and compared the results with those by a reference simulation, where the same nutrients were added

95　directly and homogeneously to the open ocean surface. They found that even if the ocean circulation remains the main driver for biogeochemical distributions in the open ocean, it appeared necessary to include riverine inputs for the representation of heterogeneous features in the coastal ocean. They identified the catchments of the tropical Atlantic, the Arctic Ocean, Southeast Asia and Indo-Pacific islands as regions of dominant contributions of riverine supplies to the ocean, leading to a strong primary production increase in the tropical west Atlantic, Bay of Bengal and the East China Sea. Nevertheless the focus here

100　was mainly on C export, and N feedbacks have not been considered by Lacroix et al. (2020).

As P concentrations have been increasing in many water bodies over the world, rivers transport more P to the coastal oceans. Beusen and Bouwman (2022) showed that human-dominated river supply of N and P has not only increased in the past, but will do so in the future, due to legacies of past nutrient management, even if efforts are made to reduce these nutrient loads. Regarding P, not only is the addition of nutrient *per se* relevant for ocean marine biogeochemistry, but the stoichiometric ratio

105　of N and P is also essential (Garnier et al., 2010; Redfield et al., 1963; Beusen and Bouwman, 2022). In the present study we have extended our experiment from Tivig et al. (2021) and include riverine supply of P in addition to N. We again aim to study the feedbacks in the N-cycle but this time face to the combined input of both limiting nutrients.

Specifically, we address the following questions:

- How does riverine N and P input together, rather than riverine N input alone, affect the representation of ocean biogeo-
110　 chemistry including marine primary production in our model?

- How does the addition of riverine P input affect specifically the N cycle and N-cycle feedbacks?

- What effect has the inclusion of riverine P fluxes specifically on marine oxygen concentrations?

To address these questions, an Earth system model of intermediate complexity (EMIC, Claussen et al. (2002)) that resolves the relevant biogeochemical feedbacks is employed. It allows the integration of a large number of processes at reduced com-

115　putational costs due to a coarser resolution and simplified assumptions, in case of UVic with respect to atmospheric dynamics. This form of model makes it possible to run millennial-scale simulations with different assumptions, allowing the analysis of processes and feedbacks operating in the climate system on such timescales (Weaver et al., 2001). Compared to the study of Tyrrell (1999), where a simple box model has been used to study the relative influences of nitrogen and phosphorus on oceanic primary production, the current study is based on a global 3D Earth system model, where the global and regional distribution

120　of N and P can be analysed in more detail. This is the prerequisite for the inclusion of river exports to the ocean, with different amounts of nutrients depending on the individual river. Hence, regional feedbacks in the N cycle and their effects on marine primary production can be assessed as well as localised biogeochemical reactions for example near oxygen minimum zones.

2 Methods

2.1 Earth system model UVic

The University of Victoria Earth System Climate model (UVic ESCM) version 2.9 (Eby et al., 2009; Weaver et al., 2001) consists of a three-dimensional (1.8° x 3.6°, 19 levels) general circulation model of the ocean, a two-dimensional, single-layer energy-moisture balance atmospheric model, a dynamic-thermodynamic sea ice model, and a terrestrial vegetation model. The atmospheric energy–moisture balance model (Fanning and Weaver, 1996) dynamically calculates heat and water fluxes between the atmosphere and the ocean, land and sea ice, and is forced by monthly climatological winds prescribed from NCEP/NCAR. The 19 vertical levels of the oceanic component, Modular Ocean Model 2 (MOM2), are 50 m thick near the surface and up to 500 m in the deep ocean. The oceanic physical settings are the same as in Keller et al. (2012). The ocean model includes a marine ecosystem module based on Keller et al. (2012) with updates as noted in Partanen et al. (2016). The ocean ecosystem and biogeochemical model is an improved NPZD (nutrient, phytoplankton, zooplankton, detritus) ecosystem model based on Schmittner et al. (2008) and includes seven prognostic variables: two phytoplankton classes (nitrogen fixing diazotrophs P_D and other phytoplankton P_O), zooplankton (Z), sinking particulate detritus (D), nitrate (NO_3), phosphate (PO_4) and oxygen (O_2) (Fig. 1). NO_3 and PO_4 are linked through exchanges with the biological variables by constant (Redfield) stoichiometry (Schmittner et al., 2008). Since diazotrophs can fix nitrogen gas dissolved in seawater, they are not limited by NO_3, while the growth of other phytoplankton is limited by NO_3 and PO_4. All phytoplankton are additionally limited by iron, light and temperature. For the current study of nitrogen cycle feedbacks it is a clear advantage, that UVic explicitly calculates diazotrophs and N_2-fixation. Keller et al. (2012) found that patterns and global amounts of modelled N_2 fixation were mostly consistent with the relatively sparse available observations (Sohm et al., 2011). The main differences are discussed within the framework of our results. See Keller et al. (2012) for a full description and evaluation of simulated marine biogeochemistry.

As in our previous study (Tivig et al., 2021) we use empirical transfer functions derived from benthic flux measurements to calculate benthic denitrification following Bohlen et al. (2012), combined with a subgrid bathymetry scheme for shallow continental shelves and other topographical features that are too fine to be resolved on the coarse UVic grid (see details in Somes et al. (2010b)).

2.2 Including riverine Nitrogen and Phosphorus

2.2.1 Global Nutrient Export from WaterSheds 2 (NEWS2)

The basic UVic model and ecosystem module do not account for riverine nutrient input. The only source of N in the ocean model consists in N_2-fixation. In Tivig et al. (2021) we included riverine N as calculated by a global, spatially explicit model of nutrient exports by rivers, NEWS2 (Mayorga et al., 2010). This second version of a system of sub-models estimates the present-day annual export yield at the river mouth for each of 6081 river catchment areas and for dissolved and particulate forms of organic and inorganic N and P, as well as dissolved organic and particulate carbon. In our model study, parameterization of riverine N fluxes is identical to Tivig et al. (2021). Since nitrate is the only nitrogen nutrient explicitly resolved in the
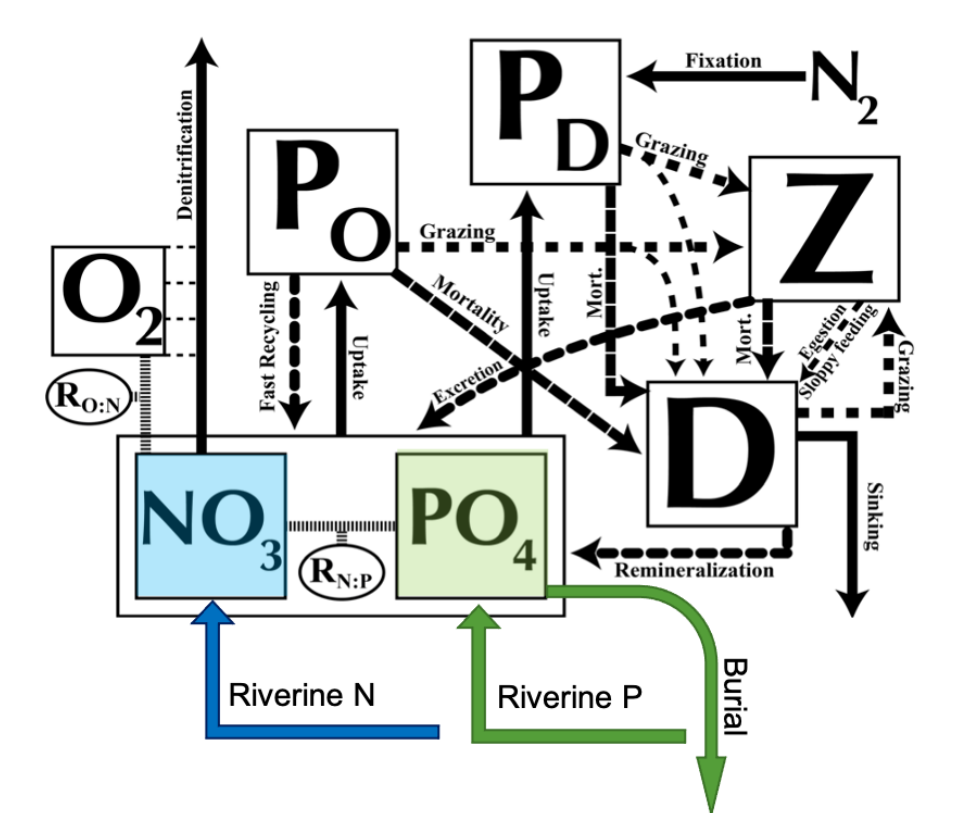
Figure 1. Ecosystem model schematics for the NPZD model with the prognostic variables (in square boxes) and the fluxes of matter between them, indicated by arrows. See details in the text. Figure updated from Keller et al. (2012) and Tivig et al. (2021).

UVic version used, all bioavailable N has been included in the nitrate compartment of the model. See Mayorga et al. (2010) for more details on the model configuration and Dumont et al. (2005) for further details on the validation of NEWS dissolved inorganic nitrogen (DIN).

2.2.2 Riverine reactive Phosphorus

Earlier applications of the UVic ESCM assumed a fixed marine P inventory (Keller et al., 2012; Oschlies et al., 2019; Schmittner et al., 2005). In addition to DIN, we here include also P from river discharge. We focus on the total amount of reactive P, i.e. that P that exchanges with the dissolved oceanic P-reservoir and thus is available for biological uptake (Filipelli, 2008; Ruttenberg, 2003). Estimates of globally integrated pre-industrial riverine supply of bioavailable P range from 0.1 Tmol P yr^{-1} to 0.3 Tmol P yr^{-1} (Kemena et al., 2019; Ruttenberg, 2003; Filipelli, 2008; Compton et al., 2000; Colman and Holland, 2000). Taking into account only dissolved inorganic P from rivers would underestimate the amount of bioavailable P from river discharge, as most studies estimate DIP export from rivers to be significantly lower, between 0.01 and 0.05 Tmol P yr^{-1} (Mayorga et al., 2010;

6

Filipelli, 2008; Harrison et al., 2005). Following the results of Colman and Holland (2000); Ruttenberg (2003), we decided to include dissolved organic and inorganic P (DOP, DIP), as well as 45 % of total particulate P (TPP). This represents the
170 upper range of the fraction of riverine TPP flux estimated as reactive-P (Ruttenberg, 2003; Colman and Holland, 2000). The numbers for DIP, DOP and PP export at the river mouths have been taken from the NEWS2 data set. DIP and DOP were taken as such, PP was multiplied by 0.45 to obtain the desired fraction of total particulate P. Consistent with Tivig et al. (2021), the nutrients from NEWS2 were interpolated onto the coarser UVic grid. We assumed a periodic seasonal cycle in runoff and that concentrations in the discharged river water are constant throughout the seasonal cycle. The annual P load is thus distributed
175 over the months using the fractions of monthly freshwater discharge as respective weights. The global amount of P we added to the UVic ocean is 0.17 Tmol P yr^{-1} (5.4 Tg P yr^{-1}), which lays in the range estimated by previous studies (Kemena et al., 2019; Ruttenberg, 2003; Benitez-Nelson, 2000). Since phosphate is the only phosphorus nutrient explicitly resolved in the UVic version used, we decided like for N to put all bioavailable P into the phosphate compartment of the model.
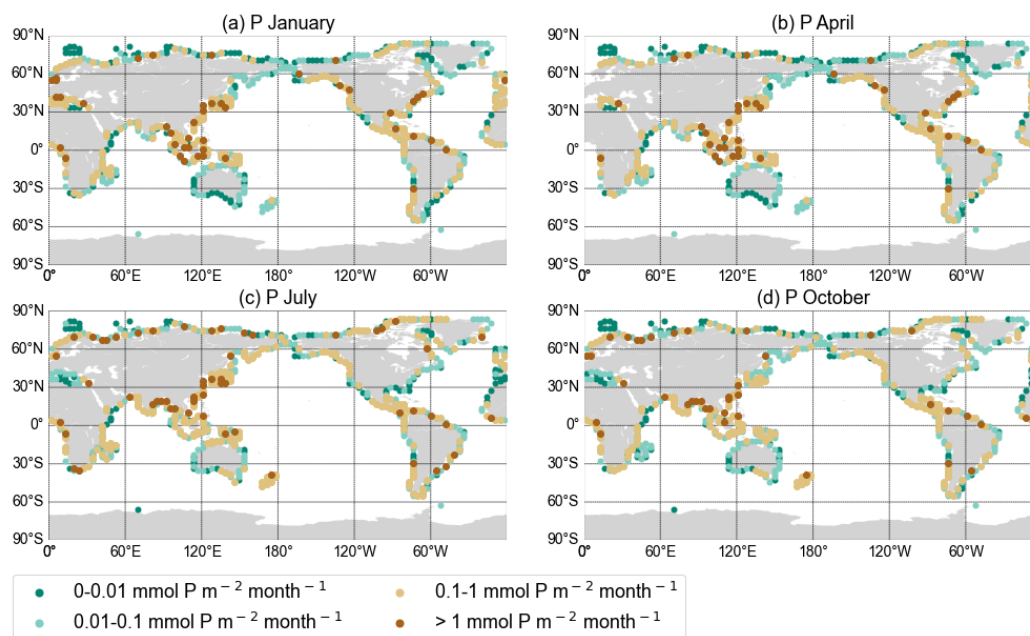
Figure 2. Export yield of total reactive phosphorus for each discharge point in mmol P m^{-2} $month^{-1}$ from NEWS2 data set interpolated on the UVic grid for January (a), April (b), July (c) and October (d).

2.2.3 Burial of Nitrogen and Phosphorus

180 In the global ocean, N input via N_2 fixation and riverine is balanced by denitrification (here implicitly including anammox). In particular denitrification in the benthic zone is considered as the major sink for fixed N (Voss et al., 2013; Galloway et al., 2004). As in Tivig et al. (2021), we include empirical transfer functions derived from benthic flux measurements (Bohlen et al., 2012)

to simulate benthic denitrification. These functions are based on dynamic vertically integrated sediment models and estimate denitrification from the rain rate of particulate organic carbon to the seafloor, bottom water O_2 and NO_3 concentrations. We

185 use a subgrid bathymetry scheme for shallow continental shelves to better resolve particulate organic matter sinking and remineralization at the seafloor (Somes and Oschlies, 2015; Somes et al., 2013).

UVic does not contain a prognostic and vertically resolved sediment model. Therefore, the input of reactive P to the ocean has to be counterbalanced by a parameterized sink. For this purpose, we include burial functions based on Flögel et al. (2011) and Wallmann (2010), which have been tested in previous studies with UVic by Kemena et al. (2019) and Niemeyer et al. (2017).

190 With these functions, the burial of P in the sediment (BUR_p) is calculated in every ocean grid box column from the difference between the simulated detritus P rain rate to the sediment (RR_p) and the benthic release flux of phosphate from the sediment (BEN_p):

$$BUR_p = RR_p - BEN_p, \tag{1}$$

Following Flögel et al. (2011), the burial of P is evaluated separately for each grid box column on the shelf and in the deep-sea.

195 Deep-sea is defined as ocean grid box columns where the ocean is deeper than 1000 m.

Benthic P release (BEN_p) is calculated locally with:

$$BEN_p = \frac{BEN_c}{r_{c/p}}, \tag{2}$$

BEN_c represents the benthic fluxes of carbon and was computed from the difference of the carbon rain-rate to the sediment (RR_c) and a virtual burial flux of organic carbon (BUR_c):

200 $$BEN_c = RR_c - BUR_c, \tag{3}$$

Depending on the ocean depth of the considered grid box, BUR_c is computed from the modelled detritus export in terms of carbon, on the shelf and continental margin (Kemena et al., 2019):

$$BUR_c = 0.14RR_c^{1.11}, \tag{4}$$

and in the deep sea:

205 $$BUR_c = 0.14RR_c^{1.05}, \tag{5}$$

RR_c is calculated by the model in mmol C m^{-2} yr^{-1}. The $r_{c/p}$ ratio depends on bottom water oxygen concentration and is calculated following Kemena et al. (2019) and Wallmann (2010):

$$r_{c/p} = Y_F - A * exp(-O_2/r) \tag{6}$$

with O_2 in mmol m^{-3} and the coefficients $Y_F = 123 \pm 24$, $A = -112 \pm 24$ and $r = 32 \pm 19$ mmol m^{-3}. Variations in the

210 coefficients determine the strength of the burial. Because there are large uncertainties in these numbers, different experiments have been performed to evaluate the model response to variations in burial.

2.3 Experimental design

To analyse the effect of riverine nutrient supply in the UVic model, six experiments were performed (Table 1). In each experiment the model was run for 10,000 years, starting from an already-spun-up steady state with the standard model version without riverine nutrients, with pre-industrial conditions for insolation and a fixed atmospheric CO_2 concentration of 283 ppm (Keller et al., 2012), i.e. a stable climate. Note that the spin-up did not include benthic denitrification and subgrid bathymetry. These two features have been included at the start of each simulation, including the control simulation (CTR). Hence, at the start of each simulations and for approximately 2000 years, there is a drift in N concentration.

Like in our previous study Tivig et al. (2021), a control simulation (CTR) was performed without riverine nutrients. The simulation NEWS-N is identical to the main experiment analysed in Tivig et al. (2021), where only DIN from river discharge was added to the coastal ocean. In a follow-up experiment, rivers exported only P to the modelled ocean (NEWS-P), but without any burial to balance the P budget. NEWS-N+P tested the impacts on marine biology and biochemistry with regard to additional N and P (without P burial). Finally, two P burial variation experiments have been performed, where riverine N and P supply from the NEWS2 model was applied. In a low burial configuration (N+P-BURLOW) we used the coefficients tested by Kemena et al. (2019) in their simulation low-bur. The second burial experiment (N+P-BURHIGH) includes the original burial functions of Flögel et al. (2011) with the coefficients for Y_F, A and r described there as well as in the reference burial experiment in Kemena et al. (2019) (Table 1).

Note that previous studies using these burial functions have balanced the modelled P budget by an equivalent weathering flux providing P to the ocean via river discharge in the same amount as P is buried in the marine sediments (Kemena et al., 2019; Niemeyer et al., 2017). In the current study there is no direct link between the two fluxes: riverine P is calculated from the NEWS2 model (Mayorga et al., 2010), while P burial is calculated independently, using only detritus export and bottom-water oxygen concentration (see Table 1 for the overview of the fluxes). In all simulations where riverine P is included, the global P budget is therefore not exactly balanced (Figure 3). While P concentration only slowly increases in the scenario with a low burial rate, the increase is stronger in the two scenarios without P burial (NEWS-P and NEWS-N+P). In the scenario with high burial rates, P concentrations decrease and the total P flux is negative. In the timeseries (Figure 3) it is also visible, that this flux is slowly increasing over the simulation and hence P inventory is following an asymptotic evolution.

These different simulations permit us to analyse the sensitivity of the N cycle feedbacks under different conditions of P supply and do not pretend to reproduce the exact reality. Furthermore, the phosphorus balance of the (pre-anthropogenic) ocean is still poorly defined and the input and output fluxes are only rudimentarily constrained (Wallmann, 2010; Föllmi, 1995).

3 Results

3.1 Phosphorus dynamics

In the four simulations with riverine P input, globally 0.17 Tmol P yr^{-1} (5.4 Tg P yr^{-1}) are added to the coastal oceans as reactive P (Figure 2). This is close to the amount estimated by Föllmi (1995), and within the range of other literature values for

Table 1. Overview of simulations and riverine nutrient fluxes:

Simulation	N-flux in Tmol N yr^{-1}	P-flux in Tmol P yr^{-1}	Description
CTR	0	0	UVic simulation without NEWS (Control)
NEWS-N	1.6	0	UVic simulation with DIN from NEWS
NEWS-P	0	0.17	UVic simulation with P from NEWS, no burial
NEWS-N+P	1.6	0.17	UVic simulation with N and P from NEWS, no burial
N+P-BURLOW	1.6	0.17	UVic simulation with N and P from NEWS, low burial configuration: $Y_F = 100.5$; $A = 90$; $r = 38$. (Kemena et al., 2019)
N+P-BURHIGH	1.6	0.17	UVic simulation with N and P from NEWS, high burial configuration: $Y_F = 123$; $A = 112$; $r = 32$ (Flögel et al., 2011)

global fluvial fluxes of bioavailable P (Kemena et al., 2019; Ruttenberg, 2003; Benitez-Nelson, 2000; Compton et al., 2000).
245   In NEWS-P and NEWS-N+P no sink of P was implemented, and these simulations are characterized by continually increasing P inventory (Figure 3). Benthic burial fluxes of P amount to 0.16 Tmol yr^{-1} in N+P-BURLOW and 0.24 Tmol yr^{-1} in N+P-BURHIGH, leading to an imbalance of +0.01 Tmol yr^{-1} and -0.07 Tmol yr^{-1} respectively.

These results range within the estimates for burial rates from observations, which globally vary around 0.2 Tmol P yr^{-1}: 0.11–0.34 Tmol P yr^{-1} in Benitez-Nelson (2000), 0.17-0.24 Tmol P yr^{-1} for Ruttenberg (2003) and 0.21 Tmol P yr^{-1} in
250   Filipelli (2008).

The highest simulated P burial fluxes can be found in coastal regions, especially in the western Pacific and Atlantic ocean (Figure A2). Simulated burial hot spots are situated in proximity to the coast of China, East Russia and Alaska, next to the eastern coast of North- and South-America and in the North Sea. There are no global observational data sets of P burial. Nevertheless, the distribution of the benthic fluxes is similar to other model studies that have used a similar algorithm (e.g.
255   Bohlen et al., 2012).

The inclusion of riverine P has a significant impact on global P concentrations. In simulation CTR without riverine nutrient supply, surface phosphate concentrations range from 0 mmol P m^{-3} in most of the western tropical and subtropical ocean basins to more than 2 mmol P m^{-3} in the Southern Ocean (Figure 4). The addition of riverine N (in NEWS-N) leads only to small changes in the surface P concentrations, in particular P declines reflecting enhanced biological processes (P uptake) in
260   the coastal oceans (not explicitly shown here). The regions with a decrease in P can be found in the shelf and coastal oceans, corresponding to the regions, where N concentrations increase in Tivig et al. (2021). Nevertheless, the magnitude of P changes is small compared to the spatial variance of surface phosphate concentrations of 0.64 mmol P m^{-3} in CTR and 0.85 mmol P m^{-3} after 10,000 years of riverine N supply in NEWS-N (0.65 mmol P m^{-3} at the start of the simulation). For simulations with inclusion of riverine P without benthic burial of P, surface P concentrations after 10,000 years of riverine P supply are much
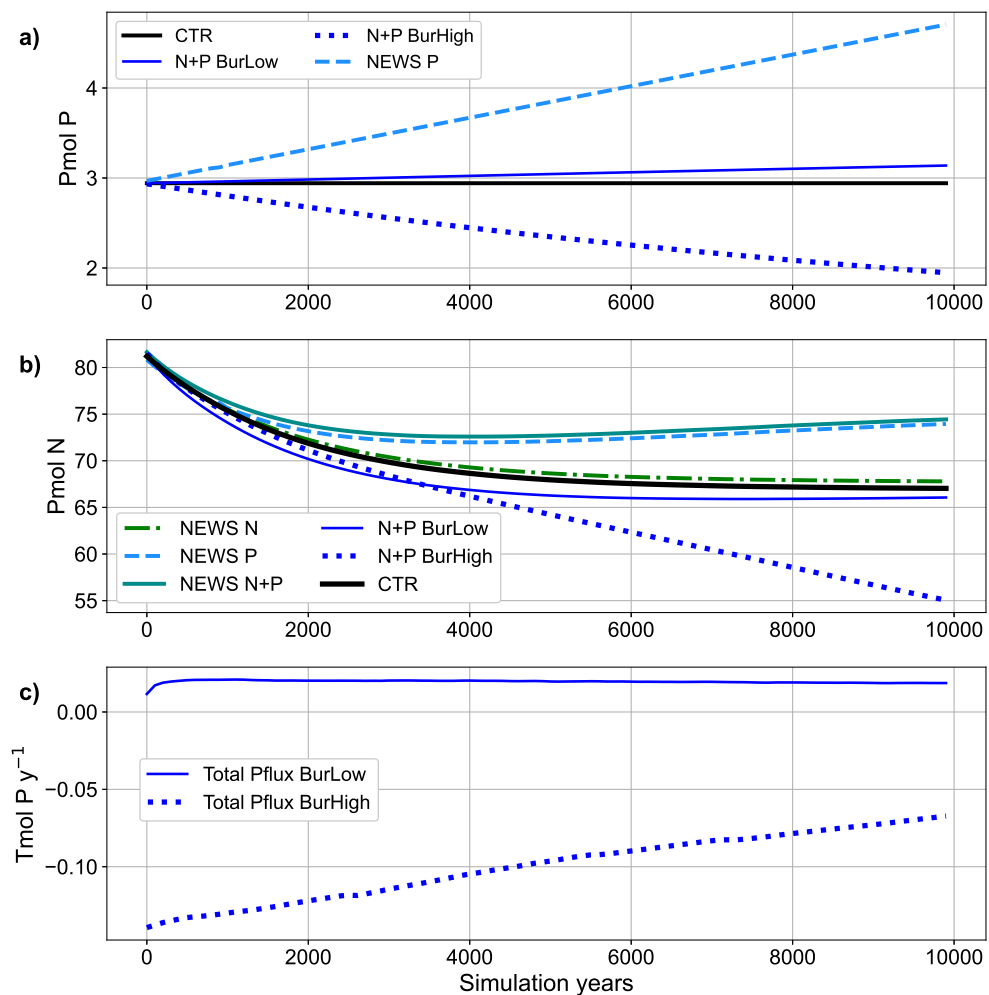
Figure 3. Top: Timeseries of global phosphorus in all simulations over the 10 000 simulation years in Pg P. Bottom: Timeseries of total phosphorus fluxes (riverine input and burial flux) in Tmol P per year for the simulations with low and high burial. Simulation descriptions can be found in Table 1.

higher than in the control simulation (Figure 4 c, d.), independent of the additional riverine N supply. Additional P is distributed over the global oceans except for the tropical Atlantic and the north-western tropical Pacific Ocean. These regions correspond to the northern subtropical gyres and are known to be oligotrophic and phosphate limited (Mather et al., 2008; Martiny et al.,

2019). The other extreme is the simulation N+P-BURHIGH, where the modelled ocean is loosing P in all those regions, where surface P concentrations are different from 0 in CTR (Figure 4 f.). Only moderate changes and a spatial variance of 0.69 mmol P m^{-3} are the result of the simulation with riverine N and P and low burial functions (N+P-BURLOW, Figure 4 e.).

After 10,000 years of simulation, of all experiments including riverine phosphate, the global average P concentration in N+P-BURLOW is nearest to observed present-day oceanic conditions (compare observations with data from the World Ocean Atlas (Garcia et al., 2019b) in Figure A4). Nevertheless, each scenario provides a different insight in marine biogeochemical feedbacks.

3.2   P influence on oceanic N inventory and N-cycle feedbacks

The addition of riverine P to the modelled ocean has a considerable impact on the distribution of simulated NO_3. At the end of CTR, NEWS-N and the simulation N+P-BURLOW, the N sink by denitrification and the N sources by N_2-fixation and riverine input are balanced (Figure 3, Figure 5). This is not the case for NEWS-P and NEWS-N+P, where the oceanic N inventory slightly increases even at the end of the simulations, and very different from N+P-BURHIGH, where N concentrations decrease continuously. This evolution is also different from P inventory, with its asymptotic shape (Figure 3). In NEWS-P, where only P is added via river runoff, global oceanic N is only slightly lower than in NEWS-N+P and considerably higher (around 6 Pmol N) than in NEWS-N. This is mainly the result of the increase in N-fixation triggered by the additional P flux (Figure 5). Comparing NEWS-N, NEWS-P and N+P-BURLOW shows, that while global benthic denitrification stays nearly constant during the simulations, water column denitrification and N_2-fixation develop differently depending on the experimental design (Figure 5): additional P leads to an increase in global denitrification and N_2-fixation. Including low burial functions stabilizes both fluxes over time, but at higher levels than in NEWS-N. In N+P-BURHIGH N-fixation and water column denitrification decrease significantly over the simulations, but seam to stabilize at the end of the 10,000 years. But the flux of benthic denitrification decreases slowlier and has not stabilized at the end of the experiment, causing the continuous N decrease in this simulation. To see a stabilized budget here, the simulations should have been much longer.

In the upper oceans, NO_3 concentrations increase with supplemental P, except near the main oxygen minimum zones (OMZ) of the Gulf of Guinea, the northern Indian Ocean and the tropical eastern Pacific . Without P burial, N increases especially in the tropical Pacific, the North Atlantic and the higher latitudes, but decreases in the tropical eastern Pacific. Including P burial leads to smaller N increase, and even a high N decrease in the simulation with high P burial (Figure 6).

Including riverine P has more impact than including riverine N supply alone. If more P is buried, N concentrations decrease globally. The above pattern of N show increasing concentrations almost everywhere in experiment NEWS-P and NEWS-N+P compared to CTR, but is almost reversed for experiment N+P-BURHIGH, with N concentrations increasing only near the OMZ in the Bay of Bengal and off the Pacific coast of Central-America (Figure 6).

These changes in NO_3 concentrations are the result of P fluxes impacting the two main processes of the N feedback-cycle, denitrification (Figure 9) and N_2-fixation (Figure 8). It is widely assumed, that the surface NO_3 to PO_4 ratio is a dominant controlling factor of these feedback mechanisms (Gruber, 2008). Diazotrophs are limited by P, especially in regions, where

12
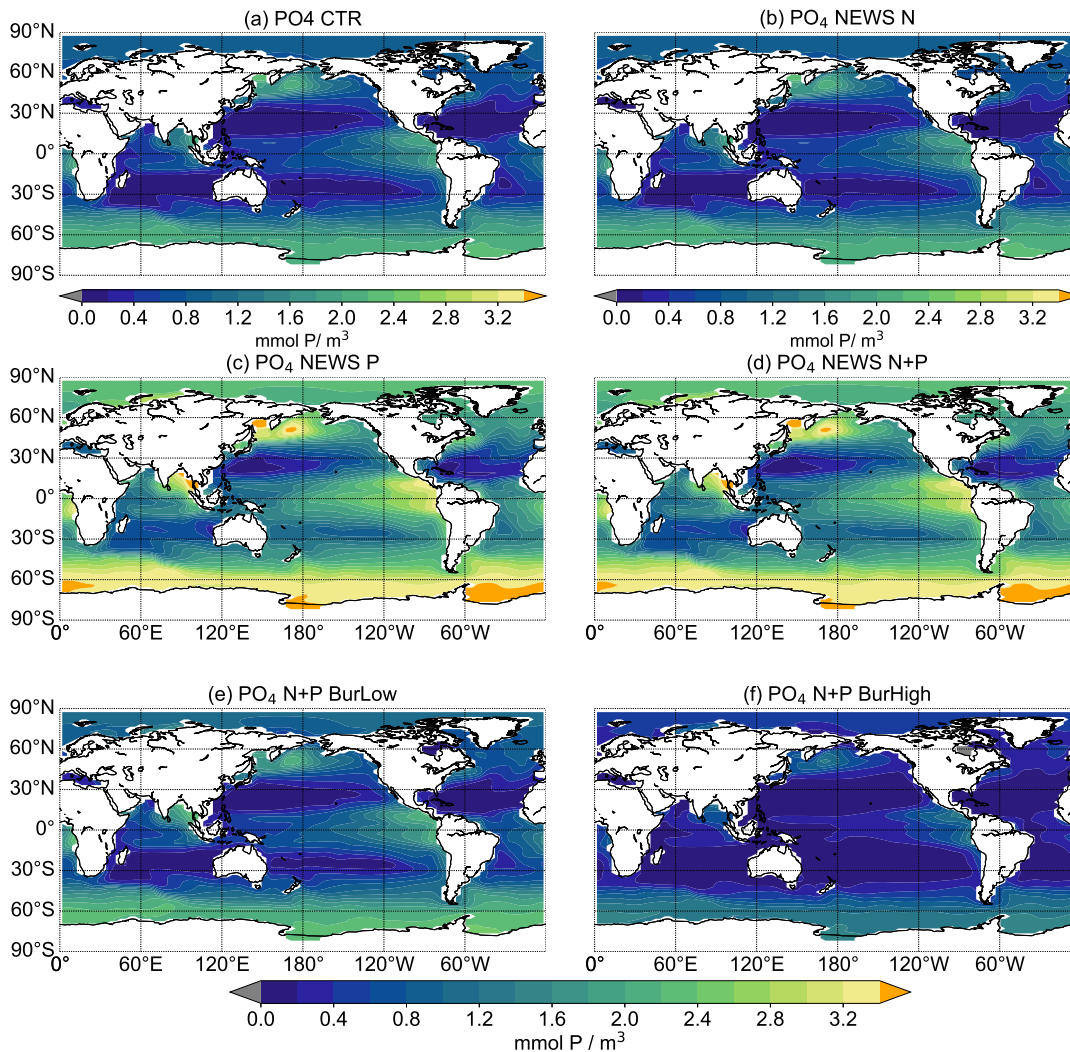
Figure 4. Global distribution of PO$_4$ concentrations in mmol P m^{-3} averaged over the upper 180 m at the end of the respective simulations over 10,000 years. (a) Global distribution of PO$_4$ concentrations in CTR (b) NEWS-N (c), NEWS-P (d), NEWS N+P (d) N+P-BURLOW (e) and N+P-BURHIGH (f). The orange colour indicates regions, where the PO$_4$ concentrations exceeds 3.4 mmol P m^{-3}.

light, temperature and iron availability are not limiting. The regions where N$_2$-fixation is enhanced in the simulations with riverine P (NEWS-P, NEWS-N+P and N+P-BURLOW) corresponds well with regions of general P limitation (compare with (Kemena et al., 2019), Figure 8). N$_2$-fixation is stimulated here by the addition of P to the ocean and is generally sensitive to changes in P supply: In the experiment with high burial rates, these same regions are charaterized by decreasing N$_2$-fixation rates (Figure 8, (f)).

305

13

Denitrification is the other feedback mechanism controlling the global ocean N budget. In the simulations where N concentration increases due to higher N_2-fixation rates, denitrification is enhanced as well. In the simulation with high P burial rates on the other hand, denitrification rates are much lower than in the control simulations in the Gulf of Guinea, the Bay of Bengal and the eastern tropical Pacific (Figure 9, (f)), leading also to higher N concentrations in these regions (Figure 6).

Both processes, N_2-fixation and denitrification, are increased in the simulation with additional riverine P. Where they take place in seperated regions of the tropical and subtropical oceans, these processes lead to an increase in N in the global surface ocean (N_2-fixation) and a loss in N in the water columns near the main OMZ of the ocean (denitrification). This is not the case for example in the Bay of Bengal.

In our previous study with the addition of only riverine N, the "vicious cycle" defined by Landolfi et al. (2013) was suspected to be the reason for a significant decrease in N concentration in the Bay of Bengal, even though rivers exported additional N to the sea (Tivig et al., 2021). Adding riverine P enhances this process here, so that the ocean is loosing N not only in the Bay of Bengal, but also in the upper tropical Atlantic ocean basin (Figure 7d,g,j,m) near the Gulf of Guinea and in the upper tropical Pacific ocean (Figure 7e,h,k,n).

The main driver for this vigorous vicious cycle in these simulations is P supply from the rivers and the interplay of different feedback loops in the marine biogeochemistry (Figure 10). Considering N on the one side, additional N from rivers or atmospheric fixation enhances marine biological production, which contributes to higher export rates, leading to remineralization and oxygen consumption. In regions, where oxygen is scarce, denitrification will take place and consume N. N_2-fixation is limited by P. Therefore, adding more P for example from rivers can enhance this process and by this the vicious cycle. On the other hand, increasing P can also lead to lower oxygen concentrations and therefore more denitrification.

Note that iron availability also plays an important role. It is a limiting factor of diazotroph growth and hence N_2-fixation (Landolfi et al., 2013). Iron availability can lead to a shift in the growth of N fixers to regions with higher iron availability, and therefore also decouple denitrification and N_2-fixation, breaking by this the vicious cycle (Landolfi et al., 2013; Moore et al., 2009). Our UVic model represents iron including a static concentration mask. Therefore no interactive response to perturbations of ocean biogeochemistry are possible and iron availability and limitation will not change during the simulations (Nickelsen et al., 2014).

3.3 Phosphorus cycling and oxygen minimum zones

Low ventilation of the water column or high rates of remineralization of organic matter can cause oxygen depleted waters. Niemeyer et al. (2017) found that the increase in the marine phosphorus inventory under assumed business-as-usual global warming conditions could lead to a 4- to 5-fold expansion of the suboxic water volume over millennial timescales. Several studies also suggest, that O_2 depletion in coastal regions caused by eutrophication may enhance P release from sediments, thereby providing additional P (Flögel et al., 2011; Wallmann, 2010; Ingall and Jahnke, 1994). These two processes together form a positive feedback loop, enhancing oxygen depletion and expansion of the oxygen minimum zones (Oschlies et al., 2018) (Figure 10). The processes relevant for this feedback are all included in the burial experiments.

Three regions, the Gulf of Guinea, the Bay of Bengal and the eastern tropical Pacific ocean are characterised by low to very low oxygen concentrations (Figure 11a).

The black contour lines in Figure 11 indicates the extent of the oxygen minimum zones at 300 m depth, averaged over the last 100 years of the simulations. The oxygen minimum zone is defined here by O_2 concentrations lower than 70 mmol m^{-3}.
The main regions with low oxygen concentrations are known to be situated in subsurface waters of the Arabian Sea and in the areas of the eastern boundary upwelling regions in the tropical oceans off California, Peru and Namibia (Oschlies et al., 2018, e.g.). The model results (Figure 11(a)) show, that UVic misplaces the oxygen minimum zone in the Indian Ocean from the Arabian Sea to the the Bay of Bengal. This is similar to other biogeochemical ocean models (Séférian et al., 2020). In reality, the Bay of Bengal is a region with strong seasonality driven by the Asian monsoon system (Löscher et al., 2020). Therefore highly variable oxygen concentrations inhibit denitrification while high water column denitrification has been observed in the Arabian Sea (Johnson et al., 2019; Bange et al., 2005).

In the simulations with increased P from rivers oxygen concentrations decrease significantly in all tropical oceans as well as in the eastern boundary regions. P burial damps the oxygen depletion and can even lead to an increase in oxygen concentrations especially in the tropical oceans and in the OMZs (Figure 11). Changes in oxygen concentrations are not limited to oxygen minimum zones and regions do not exactly correlate with regions of changed denitrification rates (Figure 9).

An observational estimate of today's suboxic water area and volume equals 30.4 ± 3 millions of km^2 and 102 ± 15 millions of km^3 respectively, for oxygen concentrations less than 20 mmol m^{-3} (Paulmier and Ruiz-Pino, 2009). In CTR, OMZ defined as regions with oxygen concentration less than 20 mmol m^{-3} (less than 70 mmol m^{-3}) extend to 13.1 millions of km^3 (52 millions of km^3). The addition of riverine N alone leads only to small changes in oxygen concentrations with a volume of OMZ of 13.2 (54) millions of km^3. Adding P leads to a strong increase in OMZ area with up to a 68 (192) millions of km^3 expansion in NEWS-N+P. With decreased P concentrations, the O_2 concentration increases globally and the global volume of suboxic waters is reduced to less than 1 (5) millions of km^3. Water column denitrification is mainly controlled by the oxygen concentration (Gruber, 2008). While adding riverine N does not impact the ocean denitrification significantly, the addition of P leads to an increase in denitrification in the three main regions with oxygen deficit waters (Figure 12). Consequently this leads also to reduced N concentrations in these same regions. However, high P burial rates worldwide and hence lower P concentrations lead to significantly higher O_2 concentrations, decreased rates of denitrification and therefore higher N concentrations. This is especially the case in in regions, where the N cycle feedbacks have limited higher N concentrations before (Figure 13 (f)). Including N from rivers only slightly impacts the O_2 distribution, but can start a negative feedback loop near oxygen minimum zones. In our first experiment this phenomenon also impacted primary production in these regions, damping a global increase in marine production compared to the control simulation. Adding P from riverine export to the modelled ocean has a higher impact on N and oxygen concentration. As O_2 plays an important role in the N feedback cycles, the impact is more significant and not only reduced to the OMZ (refer also to Figure 10).

3.4 Primary Production

In Tivig et al. (2021) we showed, that including riverine N had only limited impact on marine productivity, due at least partially to feedback reactions in the marine N cycle. Additional P changes this result significantly (Figure 14): Comparing the simulation with riverine N only to the simulation with riverine P only shows that, at least in our model and on a millennial timescale, P is more limiting for primary production than N alone. Primary production amounts to 67 Pg C yr^{-1} globally in NEWS-P compared to only 55 Pg C yr^{-1} in NEWS-N. Even in the low burial simulation, marine biology is more productive than in the simulation without riverine P addition (59 Tg C yr^{-1}). In N+P-BURHIGH on the other hand, where the ocean is deprived from P at the end of the simulation, production rates decrease in the global tropical oceans to reach a global integral 33 Pg C yr^{-1}. Only near the river mouths, where burial has not been effective yet, NPP rates are higher than in the control simulation. To summarize, NPP rates are sensitive to P addition in our model. In the simulations with N and P addition from rivers, the feedbacks are still active, but NPP rates are nevertheless higher than in our simulation with riverine N alone.

4 Discussion and limitations

In this study we compare simulations with different biogeochmical settings for N and P in the same ocean circulation. We find that the addition of riverine phosphorus to the coastal oceans in our model, has more impact on the nitrogen cycle and its internal feedbacks than the addition of N alone (Figure 10). First it impacts the N budget directly by enhancing N-fixation, especially in P limited regions. Secondly, it fuels marine primary production, which leads to an increase in detritus export and hence remineralization, which in turn reduces oxygen concentration. Lower oxygen conentration increases denitrification and therefore balances the nitrogen budget globally. We have also shown that there are regional patterns and that locally, especially in proximity of regions with low oxygen concentrations, the addition of riverine P can lead to N depletion as a consequence of a feedback loop.

Nevertheless, our experimental settings has some limitations that have to be accounted for. First, sedimentary N-loss is simulated according to an empirical transfer function based on organic carbon sinking flux to the sediments and bottom-water dissolved oxygen and nitrate. We apply the empirical function from Bohlen et al. (2012). Since our coarse resolution model does not fully resolve narrow continental shelves and coastal dynamics, a subgrid-scale bathymetry parameterization is included (Somes and Oschlies, 2015). Still, UVic underestimates sedimentary N-loss in continental shelves (see also Somes et al. (2017)). The coarse resolution of coastal regions in UVic, with no explicit simulation of the coastal processes, also implies that nutrient retention on the coastal shelf is not included. Hence, the buffer effects of the coasts is not taken into account. Riverine nutrient export to the open ocean might therefore be overestimated in our experiments. These processes could be parametrized like in Sharples et al. (2017); Izett and Fennel (2018) in a future experiment. Finally, submarine groundwater discharge to the oceans is not simulated, but might be an essential component of biogeochemical budgets (Santos et al., 2021; Slomp and Capellen, 2004).

The current study does not incorporate all the feedbacks that may potentially impact the N cycle (e.g., stoichiometric variability of phytoplankton, anthropogenically induced changes in ocean acidification and iron deposition). Also, the spatial patterns for

NPP and N_2 fixation differ from observations. In the Indian Ocean, the model simulates too much N_2 fixation in the Bay of Bengal and not enough in the Arabian Sea, a common problem of coarser resolved models, as already stated in this manuscript (Séférian et al., 2020; Moore and Doney, 2007). Of the three major quasi-permanent sites of water column denitrification (Arabian Sea, the Eastern tropical North Pacific and the Eastern tropical South Pacific off the coast of Chile (Codispoti, 2007)), the model is only able to reasonably simulate the eastern tropical North Pacific one. In the Eastern tropical South Pacific, modelled denitrification is too close to the equator and does not occur off the coast of Chile where it should (Keller et al., 2012). Nevertheless, the UVic model has been tested and used for several previous studies of marine biogeochemistry. (Keller et al., 2012) has found, that surface nitrate and phosphate concentrations are similar to observational data (Garcia et al., 2019a). The model rates of N_2 fixation are within the wide range ($\sim$ 7-15 Tmol N yr-1) of global N_2 fixation estimates (Codispoti, 2007; Deutsch et al., 2007; Gruber and Sarmiento, 1997; Karl et al., 2002). Despite the model limitations mentioned before, the University of Victoria Earth System Climate Model of intermediate complexity is a useful tool to investigate long-term changes in marine biogeochemistry and has been used and evaluated in many studies before (e.g. Mengis et al., 2020; Somes et al., 2017; Keller et al., 2012).

For the riverine nutrient input, we used the results of the NEWS2 model. Mayorga et al. (2010) and Dumont et al. (2005) evaluated the individual models for the river export and found, that despite uncertainties associated with model inputs, nutrient yield and export were close to observations and the global export estimates were similar to previous publications.

Although the riverine nutrient export from NEWS2 includes the anthropogenic component, based on the year 2000, we did not focus on the question in our experiment and the millennial-scale simulations do not provide much insight into the short time variability. Nevertheless, the question of the influence of human activities on the marine N cycle is most central. Human activities have markedly altered the earth's cycles of the nutrients nitrogen and phophorus. Beusen and Bouwman (2022) have shown that rivers, which have more than 50 % anthropogenic sources and at the same time elevated N:P ratios (> 25) contributed 36 % to the total global N export to coastal waters. They also found, that from 1970 to 2015, global N and P delivery to surface waters has increased from 44 to 71 Tg N yr^{-1} for N (3.1 to 5.1 Tmol N yr^{-1}) and 7.1 to 9.7 Tg P yr^{-1} (0.23 to 0.31 Tmol P yr^{-1}) for P, although the export has been decreased in industrialized countries. Changes do not only affect the absolute amount of the nutrients, but also the N:P ratios. Understanding the interplay between these to nutrients is therefore important, to predict changes in coastal and global oceans (Beusen and Bouwman, 2022).

5 Conclusions

In a previous study, Tivig et al. (2021) added a new component to the global Earth system model UVic, to simulate the effects of N supply from river discharge. They found that, internal feedbacks in the nitrogen cycle mostly compensated for the imposed yearly addition of 1.6 to 3.3 Tmol of riverine nitrogen and limited the impact on global marine productivity to <2 %. In the current study, riverine phosphorus has been included separately and in addition to N. After 10,000 years, only a simulation with low P burial rates reached a steady state. After 10,000 years of simulations, the global amount of P in the ocean has increased significantly in the simulations where riverine P is not balanced by burial sinks and continues to increase. In the simulation with

low burial rates, global P increases only slightly, while the simulation with high burial rates leads to a continual loss in global P. The simulations showed that, on millennial timescales, including riverine P in the model has more impact on the modelled marine biogeochemistry and biology than the inclusion of N alone. Therefore, we can answer the questions raised at the start:

– Additional P from river runoff affects marine biology not only near the river mouths but also in regions far off the coasts and in the deep oceans.

– Because the additional P (as well as the loss of P in N+P-BURHIGH) affects the two processes denitrification and N_2-fixation, the N-cycle is also affected and N concentration increases or decreases locally and globally. In simulations where P is added without burial, N concentrations also increase globally, except in regions where denitrification is dominant, in proximity to regions with low to very low oxygen concentrations. Balancing the addition of P by P burial leads to a decrease in the global marine N concentration. The global amount of N at the end of the 10,000 years is lower in the burial simulations than in the simulations without P compensation. This can be attributed to the internal feedbacks: additional P increases N_2-fixation but also denitrification. Knowing that denitrification consumes 7 mol of NO_3 for every mole of organic N provided by N_2-fixation, in regions with low oxygen concentration, a 'vicious cycle' leads to a runaway loss of N. In the simulations where P is not limiting, the N loss can be globally compensated by N_2-fixation in other regions. Where P is reduced because of sedimental burial, even if only low, N_2-fixation is not effective enough to compensate for the loss in N due to denitrification.

– Adding P in the coastal oceans has significant impact on marine oxygen concentrations. Simulated oxygen concentrations decrease globally but more in the tropical and Nordic oceans, if P is added without an additional sink. In the simulation where P is lost due to sediment burial, however, O_2 concentrations increase in the whole oceans. In Tivig et al. (2021) we found, that O_2 concentrations is only slightly impacted by the addition of riverine N alone.

Finally, our study showed that additional P from riverine input strongly influences marine productivity not only in the coastal oceans, but also in the open oceans worldwide. Our model simulations suggest that, on millennial timescales, the impact of riverine P on ocean biogeochemistry is more important than the one of riverine N. While this result is linked to our model configuration, with all its limitations described before, it confirms the conclusion of e.g. Tyrrell (1999). In our experiments we also showed that internal feedbacks in the N and P cycle play a crucial role for marine biogeochemistry and can highly impact regional biology, especially in the coastal oceans.

The main sources of P as the "ultimately limiting nutrient" are rivers transporting P provided by weathering and human activities (Giraud et al., 2008; Föllmi, 1995). While weathering processes are active on millennial timescales and therefore only slowly change the amount of P advected by the rivers, human activities have influenced these nutrient transports more rapidly during the last centuries (Beusen et al., 2016). Additionally, changes in atmospheric carbon dioxide concentrations and resulting climate changes have already and will in the future impact riverine export as well as ocean biogeochemistry (Gao et al., 2023). Although the uncertainties in the real and the modelled nutrient fluxes are still large, our simulation suggests that global ocean biogeochemistry can be affected by the supply of nutrients from rivers and that the global representation

18

of biological activity may be improved by considering riverine export and coastal processes. For this purpose, a better spatial resolution of the coastal oceans as well as more realistic representation of coastal N and P cycling processes could be helpful, also in order to analyse the variability on shorter timescales.

Appendix A: Supplemental Figures
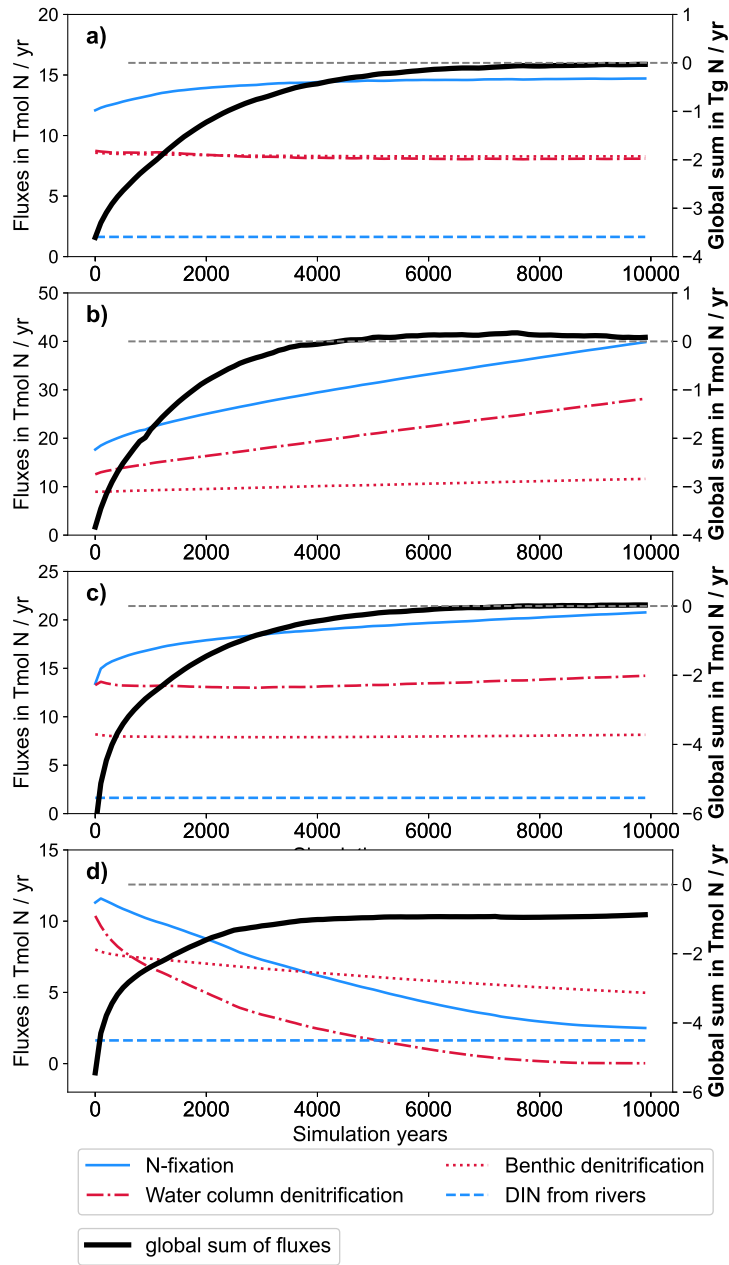
Figure 5. Timeseries of global nitrogen fluxes from NEWS-N (a), NEWS-P (b), N+P-BURLOW (c) and N+P-BURHIGH (d) over the 10,000 simulation years in Tmol N per year. Nitrogen fixation (blue solid line) and riverine N input (blue dotted line) are balanced by water column denitrification and benthic denitrification (red solid and red dotted line, respectively). The global sum of all N fluxes is shown as bold black line. Fluxes are given in absolute values. Note the different scales of y-axis. The dotted line in grey is the zero-line of the global sum of N fluxes.

20
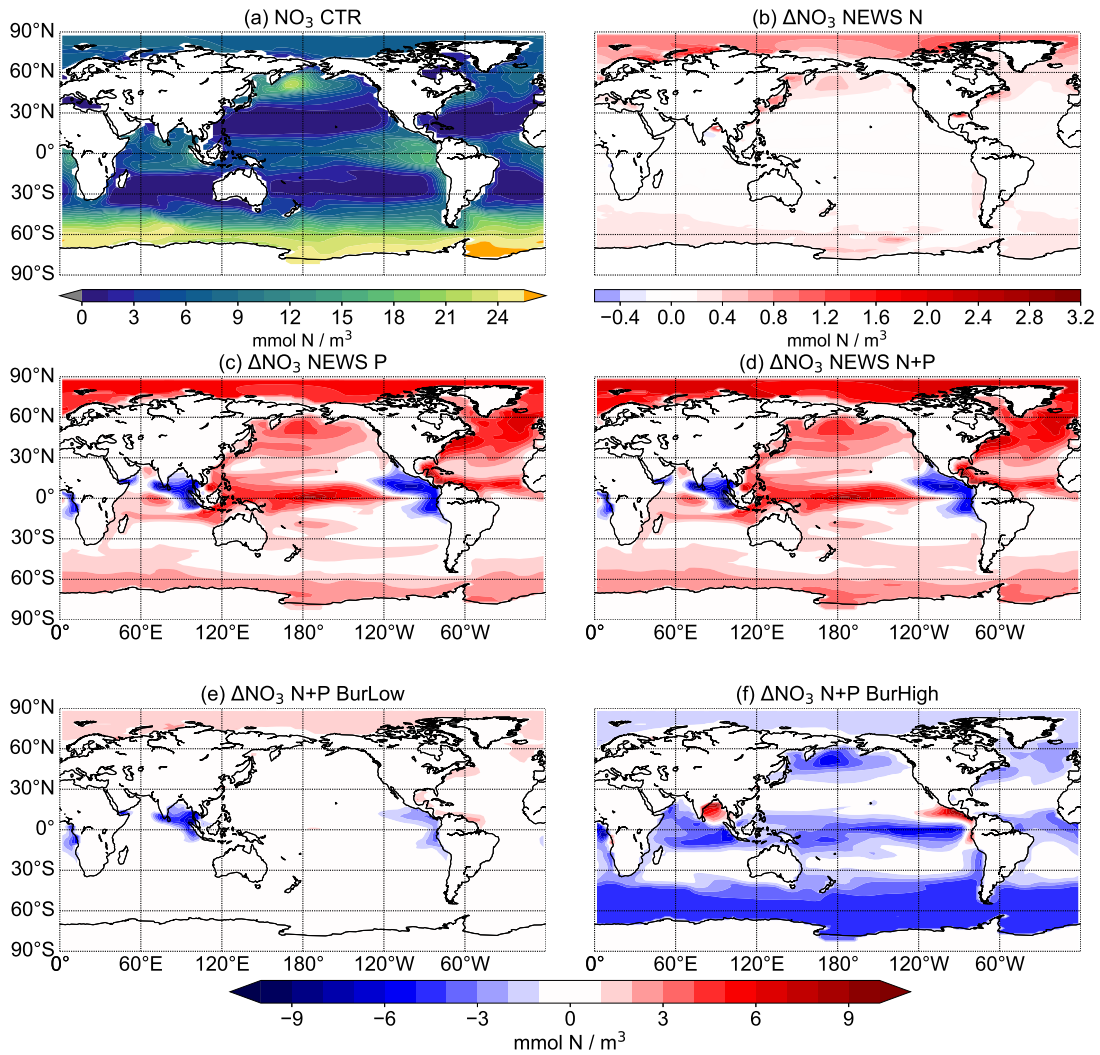
Figure 6. Global distribution of NO_3 concentration averaged over the upper 180 m in mmol N m^{-3}. The panel (a) shows NO_3 concentration in CTR. Panels (b)-(f) show N concentration in the simulations NEWS-N, NEWS-P, NEWS-N+P, N+P-BURLOW and N+P-BURHIGH as difference to CTR.
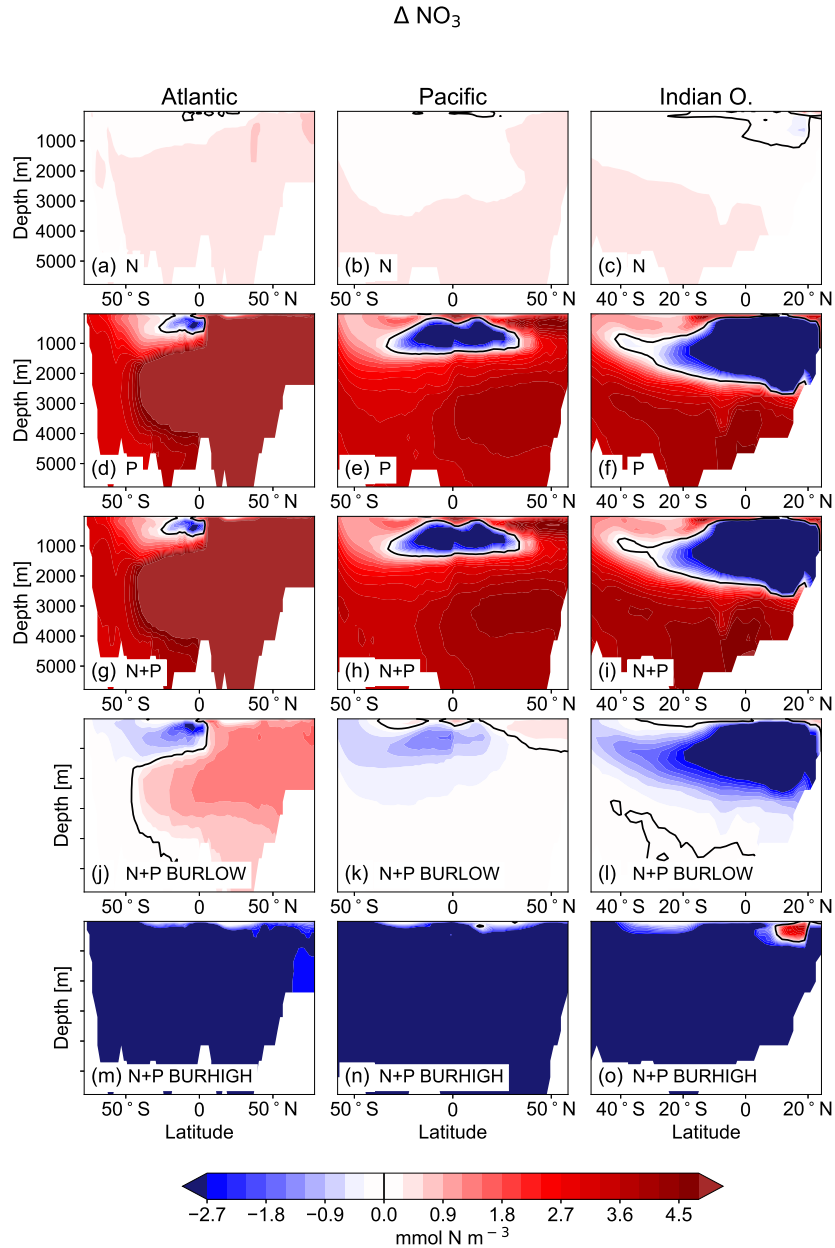
Figure 7. Difference in the zonal mean concentrations of NO₃ in the main ocean basins (Atlantic: left column, Pacific: middle, and Indian Ocean: right) in mmol N m^{-3} as difference between the simulations NEWS-N, NEWS-P, NEWS-N+P, N+P-BURLOW and N+P-BURHIGH and CTR.
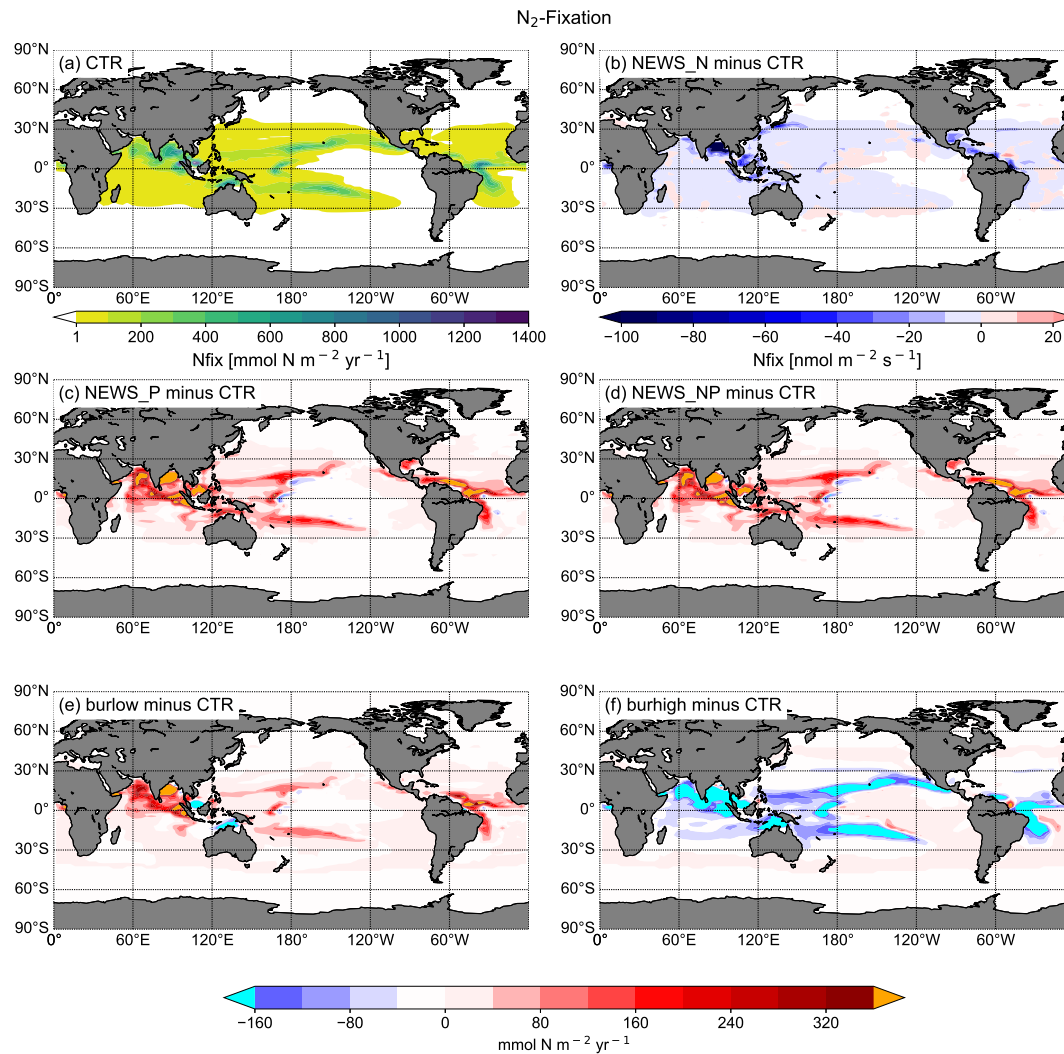
Figure 8. Vertical integration of N_2 fixation in mmol N m^{-2} yr^{-1}. (a) N_2 fixation in CTR. (b)-(f) difference in N_2 fixation between the simulations NEWS-N, NEWS-P, NEWS-N+P, N+P-BURLOW and N+P-BURHIGH and CTR. The cyan colour indicates regions with very low N_2 fixation rates compared to CTR. The orange colour indicates regions with very high N_2 fixation rates compared to CTR.

Denitrification

(a) CTR [mmol N m^{-2} yr^{-1}]

(b) NEWS_N minus CTR

(c) NEWS_P minus CTR

(d) NEWS_NP minus CTR

(e) NEWS_NP_burlow minus CTR

(f) NEWS_NP_burhigh minus CTR
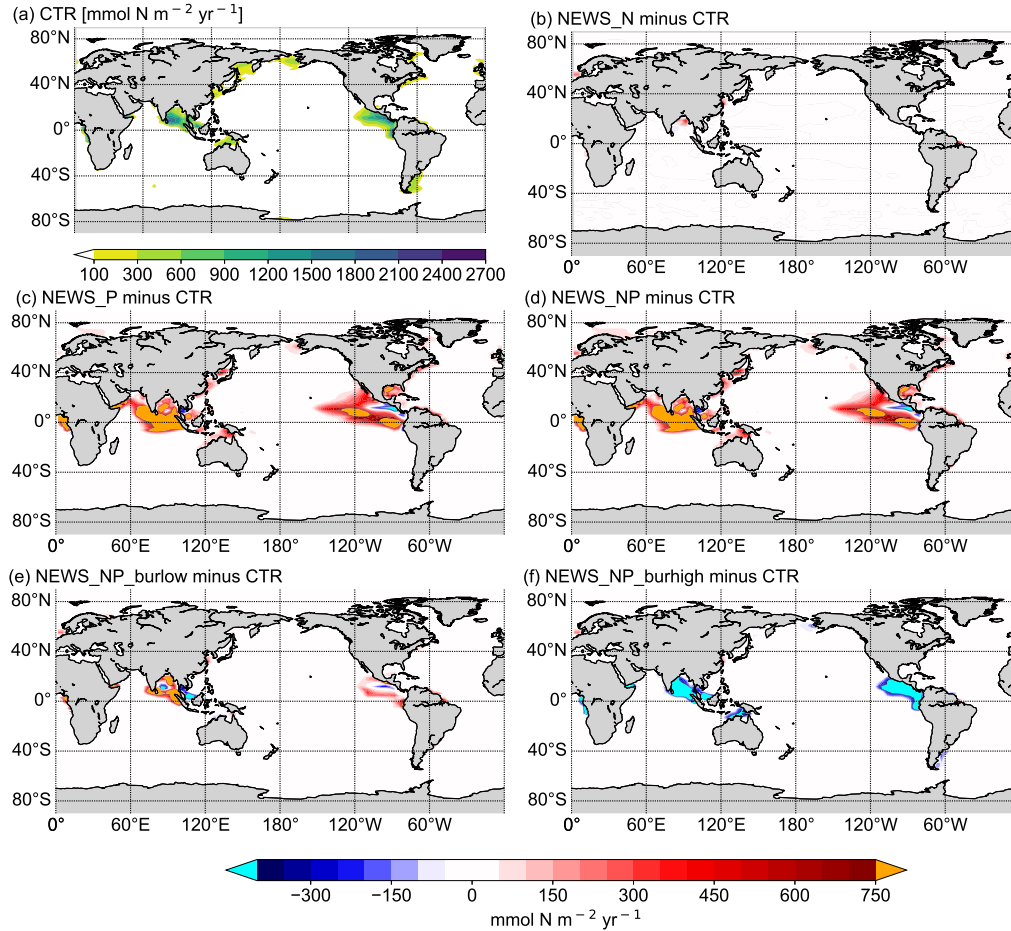
mmol N m^{-2} yr^{-1}

Figure 9. Vertical integration of denitrification in mmol N m^{-2} yr^{-1}. (a) Denitrifications rates in CTR. (b)-(f) difference in denitrification rates between the simulations NEWS-N, NEWS-P, NEWS-N+P, N+P-BURLOW and N+P-BURHIGH and CTR. The cyan colour indicates regions with very low denitrification rates compared to CTR. The orange colour indicates regions with very high denitrification rates compared to CTR.

24
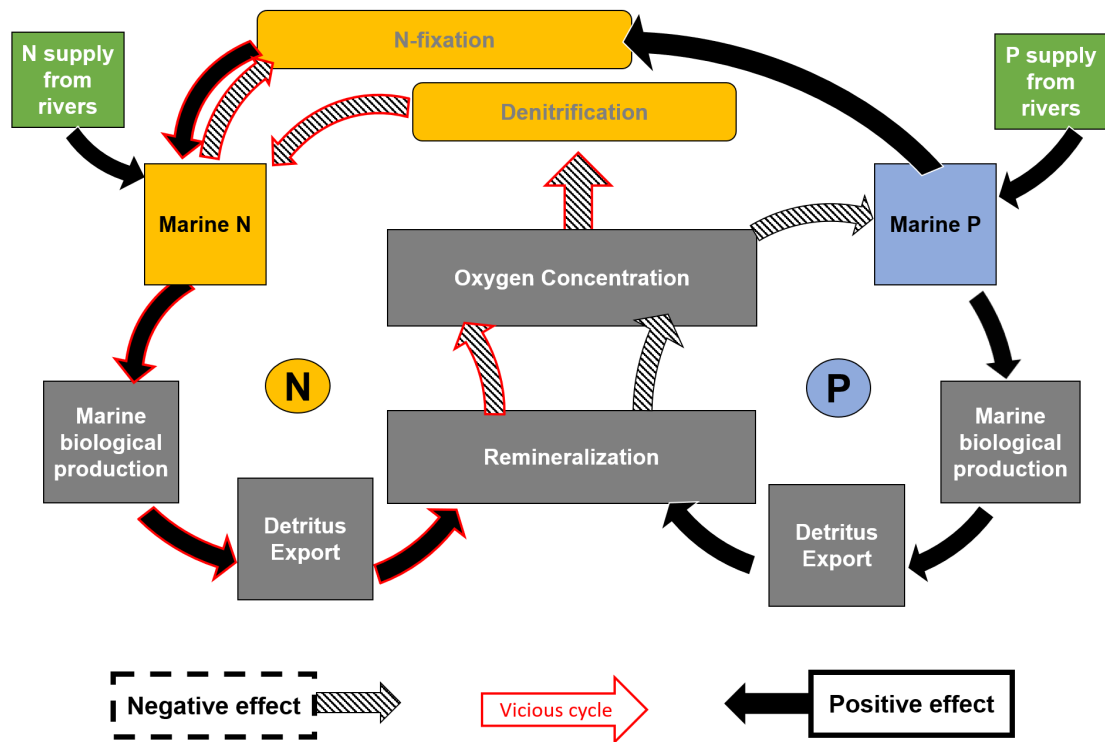
Figure 10. Feedbacks in the marine N and P cycle, due to riverine nutrient supply to the global oceans. Yellow colored boxes refer to processes concerning the marine N inventory. Blue refers to the marine P inventory. Green boxes show riverine nutrient input. The black arrows symbolise positive effects or feedbacks. The dashed arrows symbolise negative effects or feedbacks. Red bordered arrows symbolise processes involved in the vicious cycle (Landolfi et al., 2013).
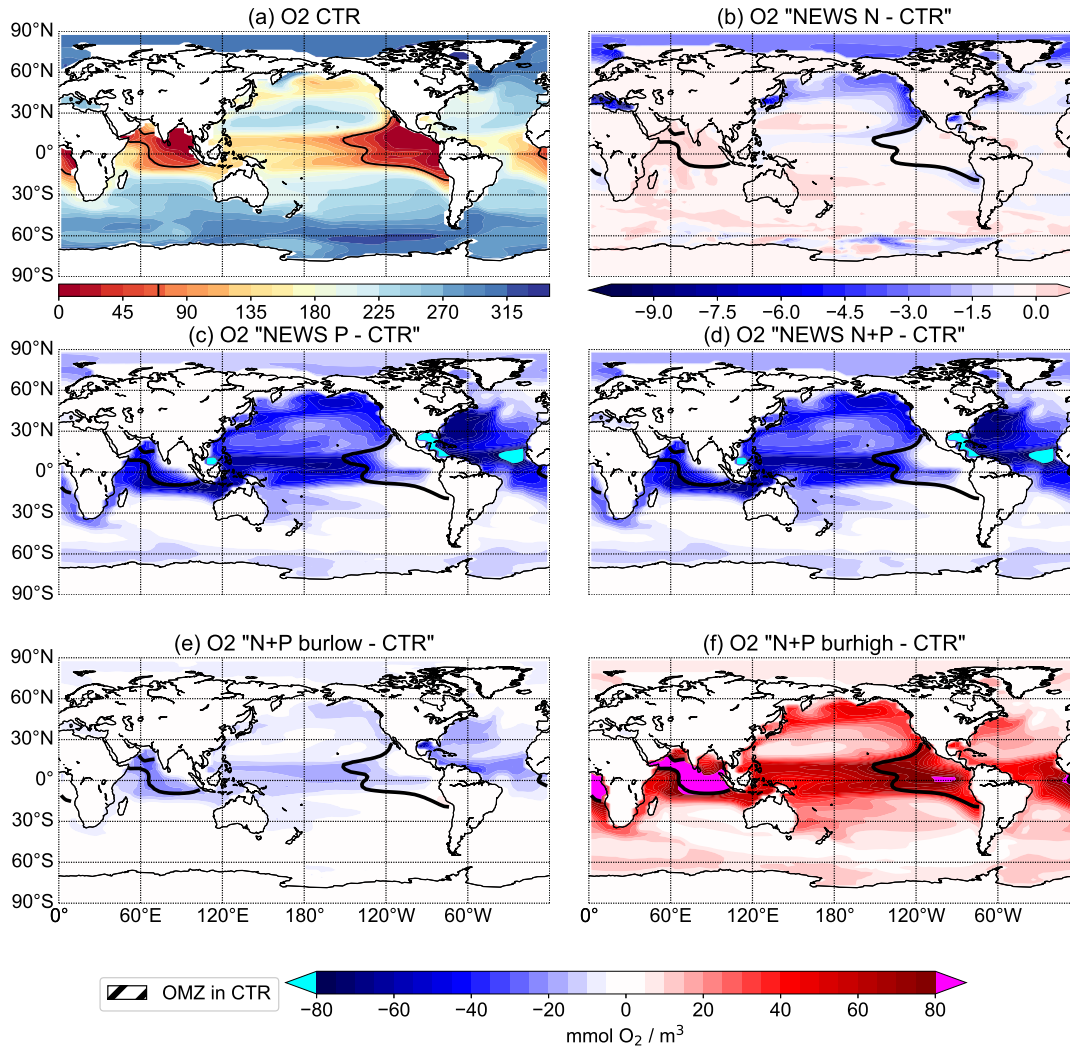
Figure 11. Oxygen concentration at 300 m depth in mmol O_2 m^{-3}. (a) distribution of oxygen concentration in the control simulation, difference in oxygen concentration between the simulations NEWS (b), NEWS-P (c), NEWS-N+P (d), PP N+P-Burlow (e), PP N+P-Burhigh (f), respectively, and CTR. The black bold line shows the limits of the oxygen minimum zone at 302 m depth in the control simulation.
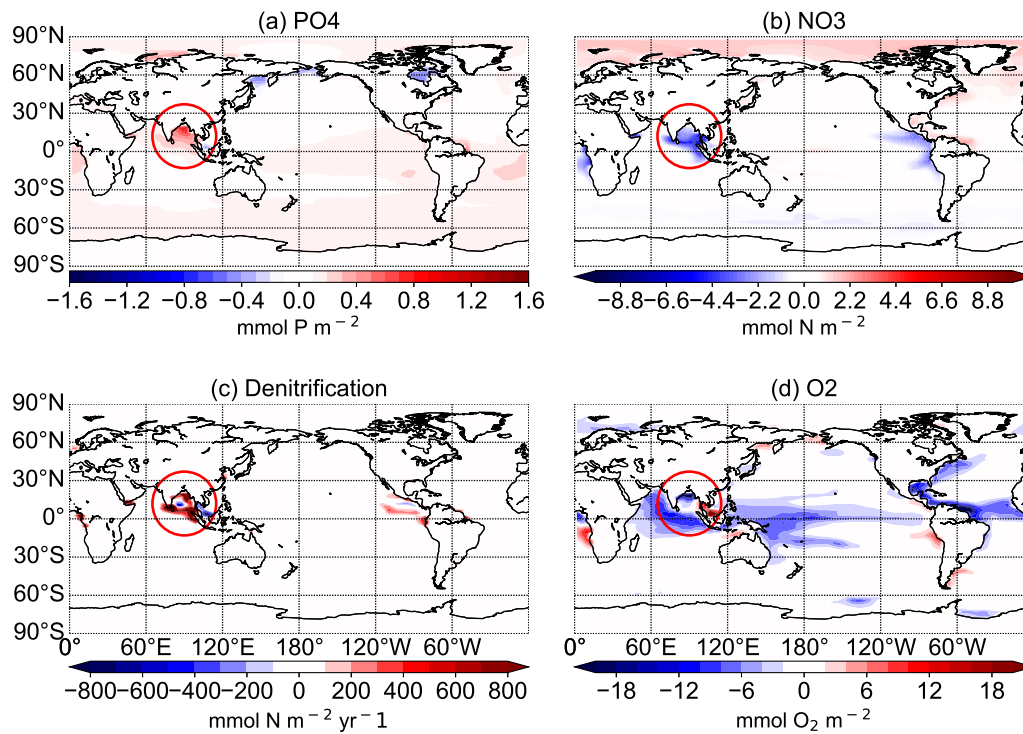
Figure 12. Difference between N+P-Burlow and CTR simulation for the average of the upper 300 m for PO_4 concentrations in mmol P m^{-3}(a), NO_3 concentrations in mmol N m^{-3} (b) and O_2 concentrations in mmol O_2 m^{-3} (d) and for the vertical integration of denitrification in mmol N m^{-2} yr^{-1} (c) at the end of the respective simulations over 10,000 years. The red circle shows the region of the Bay of Bengal.
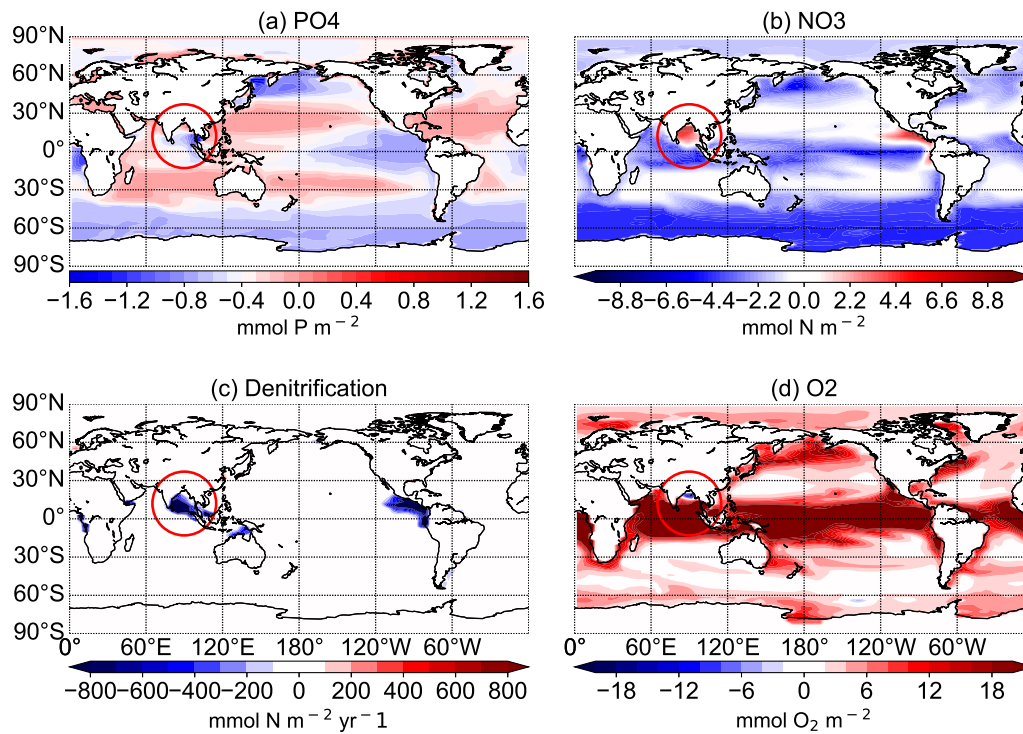
Figure 13. Difference between N+P-Burhigh and CTR simulation for the average of the upper 300 m for PO_4 concentrations in mmol P m^{-3}(a), NO_3 concentrations in mmol N m^{-3} (b) and O_2 concentrations in mmol O_2 m^{-3} (d) and for the vertical integration of denitrification in mmol N m^{-2} yr^{-1} (c) at the end of the respective simulations over 10,000 years. The red circle shows the region of the Bay of Bengal.
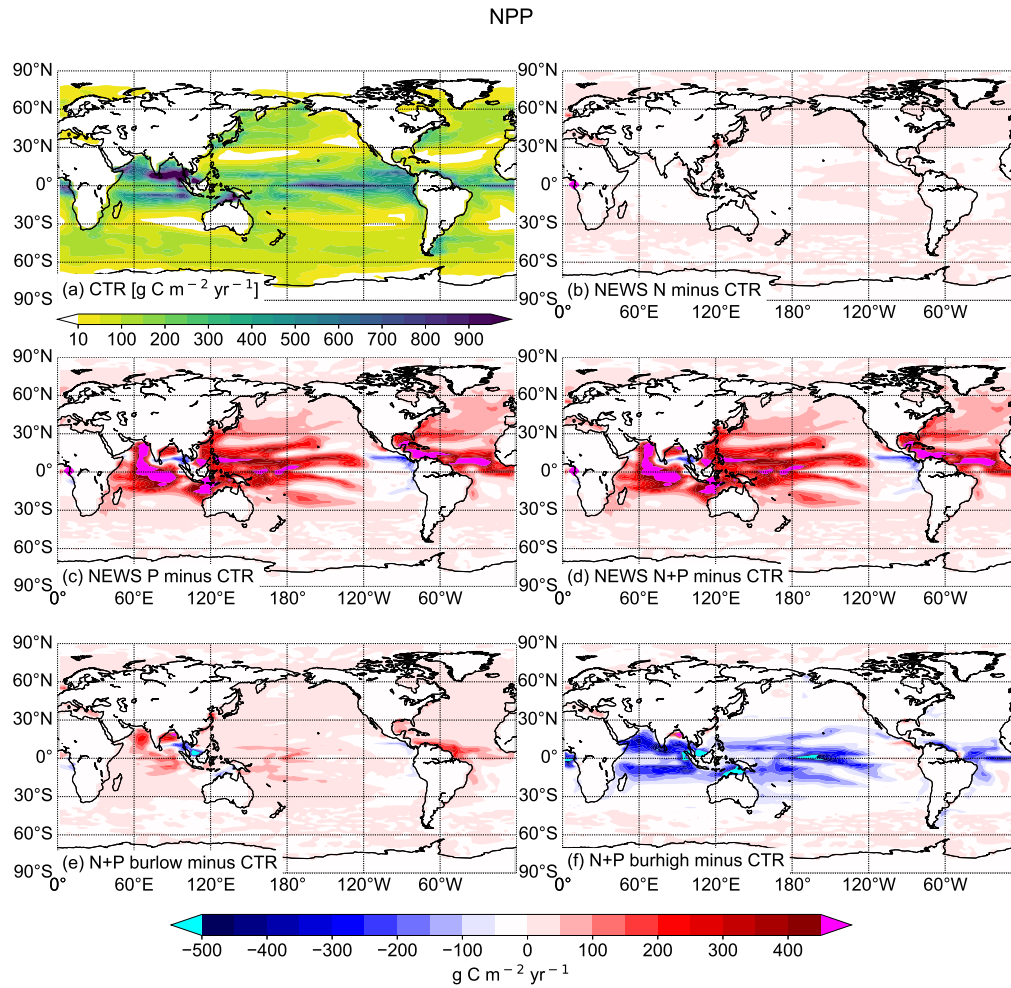
Figure 14. Vertical integration of primary production in g C m^{-2} yr^{-1}.
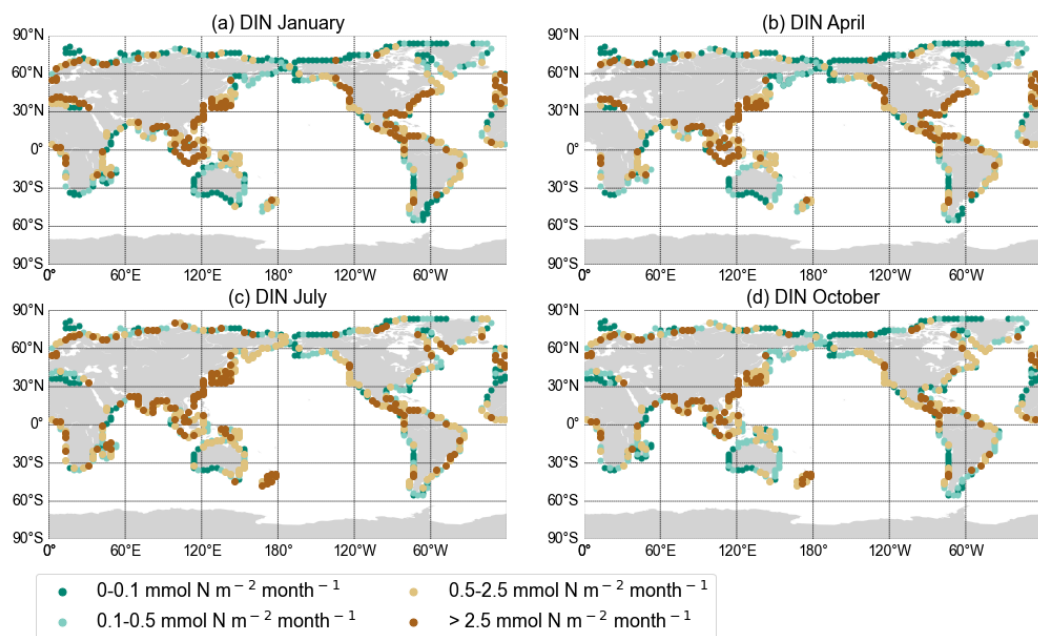
Figure A1. DIN export yield for each discharge point in mmol N m^{-2} month^{-1} from NEWS2 data set interpolated on the UVic grid for January (a), April (b), July (c) and October (d).

NEWS High Burial

mmol P m^{-2} yr^{-1}
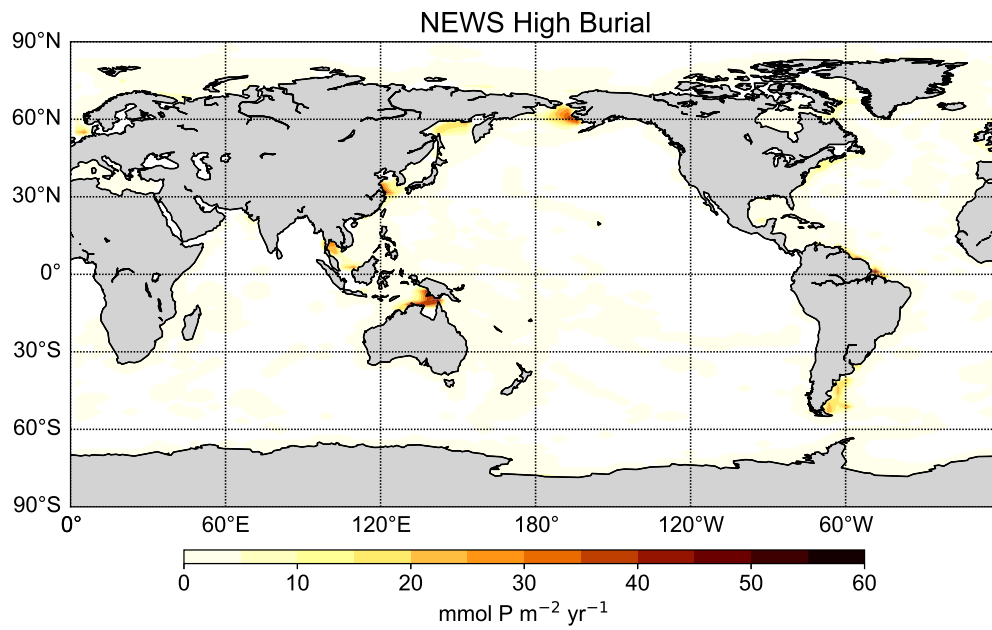
Figure A2. Burial flux of P in the N+P-BURHIGH simulation in mmol P yr^{-1}.
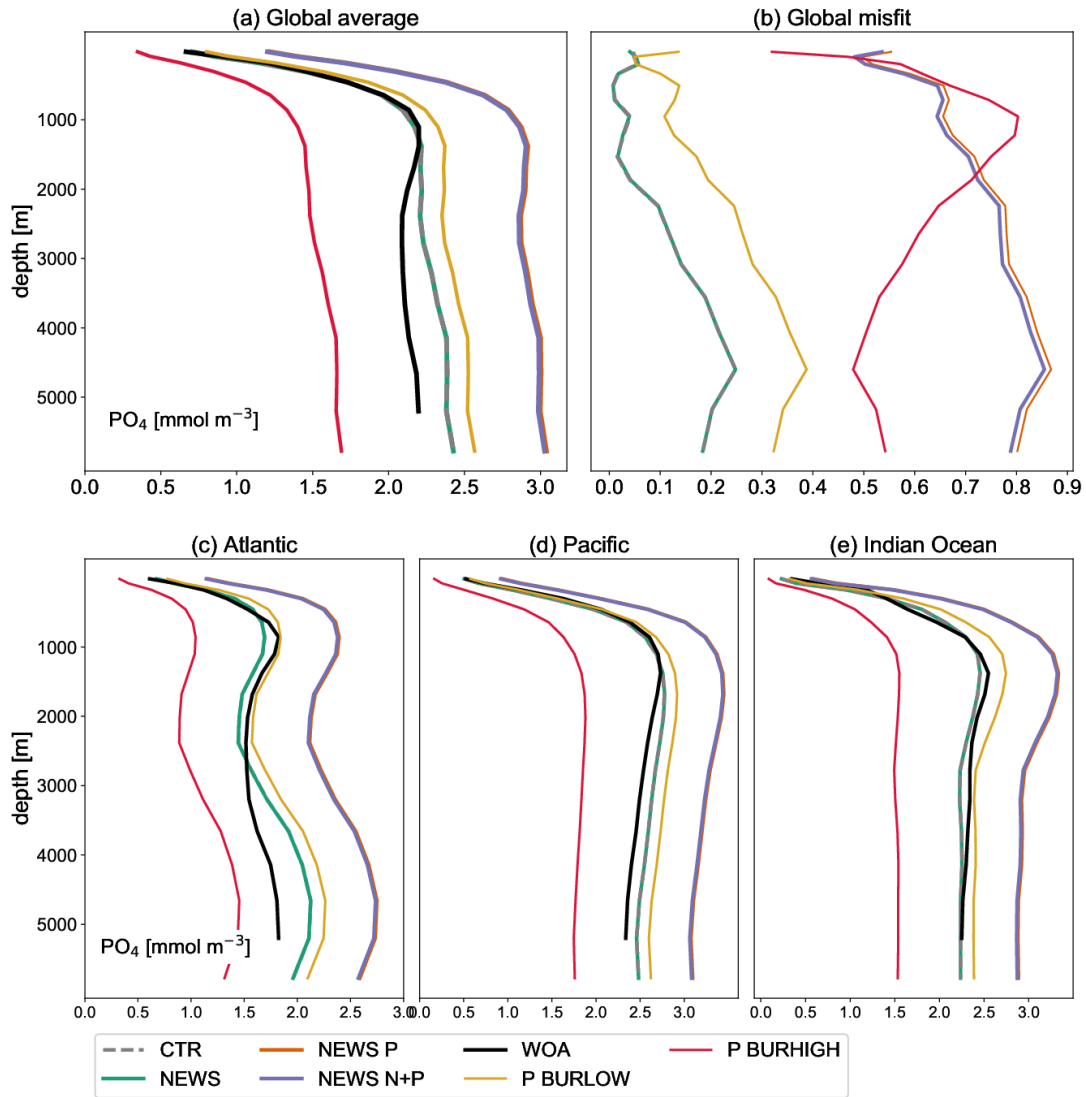
Figure A3. Global profile of PO_4 in mmol m^{-3} in the simulations NEWS, CTR, NEWS-P, NEWS-N+P, NEWS-Burlow, News-Burhigh and from the World Ocean Atlas (WOA). (a) global average of PO_4 (b), Global profiles of misfit between each simulation and the WOA dataset (c), global average profiles of PO_4 in the Atlantic Ocean (d), global average profiles of PO_4 in the Pacific Ocean (e), global average profiles of PO_4 in the Indian Ocean (f).
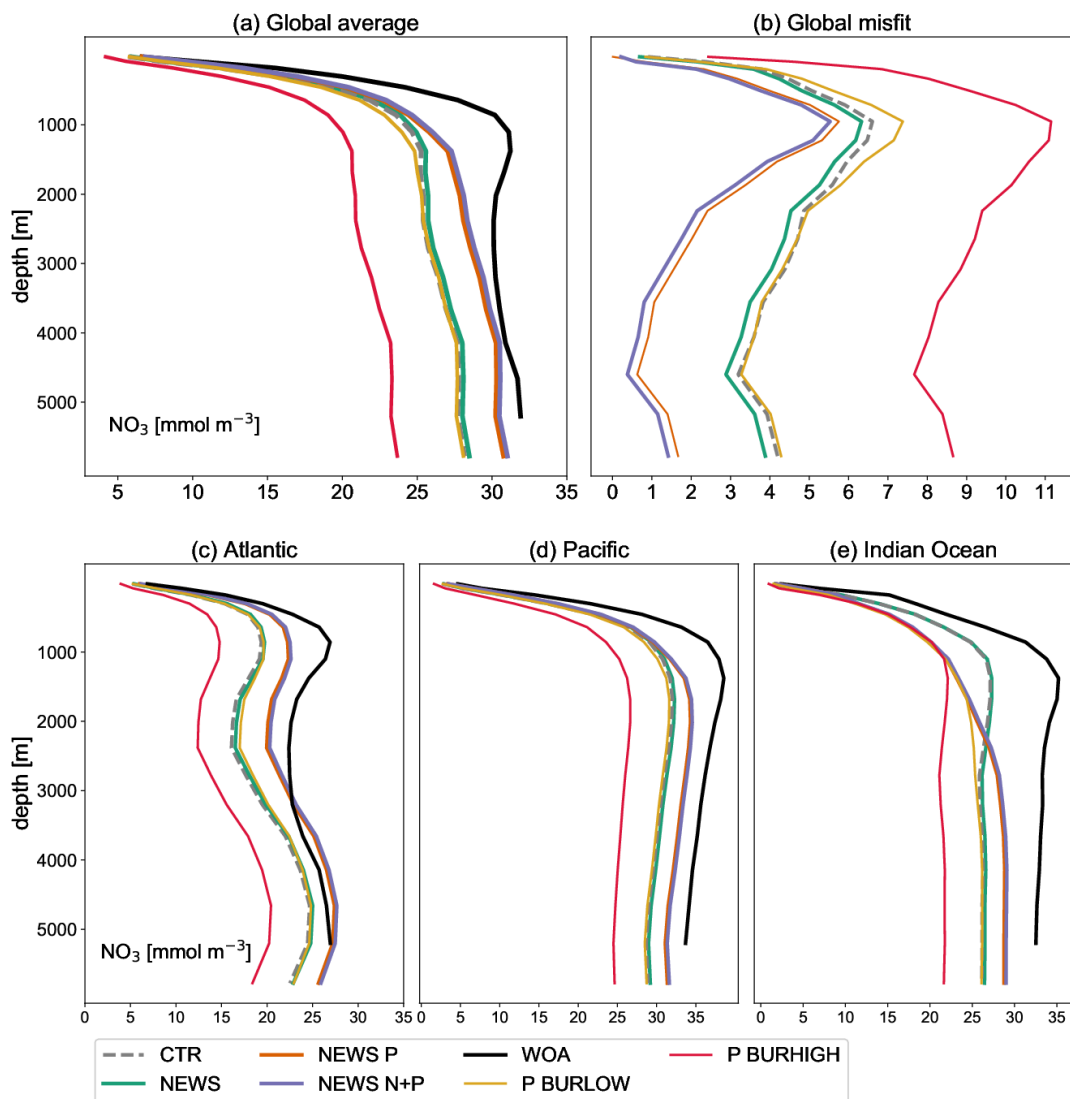
Figure A4. Global profile of NO_3 in mmol m^{-3} in the simulations NEWS, CTR, NEWS-P, NEWS-N+P, NEWS-Burlow, News-Burhigh and from the World Ocean Atlas (WOA). (a) global average of NO_3 (b), Global profiles of misfit between each simulation and the WOA dataset (c), global average profiles of NO_3 in the Atlantic Ocean (d), global average profiles of NO_3 in the Pacific Ocean (e), global average profiles of NO_3 in the Indian Ocean (f).

References

Allaby, M.: Liebig's law of the minimum, https://doi.org/10.1093/acref/9780199567669.013.3219, 2010.

495 Altabet, M. A.: Constraints on oceanic N balance/imbalance from sedimentary 15N records, Biogeosciences, 4, 75–86, https://doi.org/10.5194/bg-4-75-2007, 2006.

Bange, H., Naqvi, S., and Codispoti, L.: The nitrogen cycle in the Arabian Sea, Progress in Oceanography, 65(2-4), 145–158, https://doi.org/10.1016/j.pocean.2005.03.002, 2005.

Baturin, G. N.: Phosphorus Cycle in the Ocean, Lithology and Mineral Resources, 38, 101–119, 2003.

500 Benitez-Nelson, C. R.: The biogeochemical cycling of phosphorus in marine systems, Earth-Science Reviews, 51, 109–135, https://doi.org/10.1016/S0012-8252(00)00018-0, 2000.

Beusen, A. H. W. and Bouwman, A. F.: Future projections of river nutrient export to the global coastal ocean show persisting nitrogen and phosphorus distortion, Frontiers:Water, 4, 893 585, https://doi.org/10.3389/frwa.2022.893585, 2022.

Beusen, A. H. W., Bouwman, A. F., Beek, L. P. H. V., Mogollon, J. M., and Middelburg, J. J.: Global riverine N and P transport to

505 ocean increased during the 20th century despite increased retention along the aquatic continuum, Biogeosciences, 13, 2441–2451, https://doi.org/10.5194/bg-13-2441-2016, 2016.

Bohlen, L., Dale, A. W., and Wallmann, K.: Simple transfer functions for calculating benthic fixed nitrogen losses and C:N:P regeneration ratios in global biogeochemical models, Global Biogeochemical Cycles, 26, GB3029, https://doi.org/10.1029/2011GB004198, 2012.

Cappellen, P. V. and Maavara, T.: Rivers in the Anthropocene: Global scale modifications of riverine nutrient fluxes by damming, Ecohydrol-

510 ogy & Hydrobiology, 16, 106–111, 2016.

Claussen, M., Mysak, L. A., Weaver, A. J., Crucifix, M., Fichefet, T., Loutre, M.-F., Weber, S., Alcamo, J., Alexeev, V., Berger, A., Calov, R., Ganopolski, A., Goosse, H., Lohmann, G., Lunkeit, F., Mokhov, I., Petoukhov, V., Stone, P., and Wang, Z.: Earth System Models of Intermediate Complexity: Closing the Gap in the Spectrum of Climate System Models, Climate Dynamics, 18, 579–586, https://doi.org/10.1007/s00382-001-0200-1, 2002.

515 Codispoti, L. A.: Is the ocean losing nitrate?, Nature, 376, 1995.

Codispoti, L. A.: An oceanic fixed nitrogen sink exceeding 400 Tg Na-1 vs the concept of homeostasis in the fixed-nitrogen inventory, Biogeosciences, 4, 233–253, 2007.

Codispoti, L. A., Brandes, J. A., Christensen, J. P., Devol, A. H., Naqvi, S. A., Paerl, H. W., and Yoshinari, T.: The oceanic fixed nitrogen and nitrous oxide budgets: Moving targets as we enter the anthropocene?, Scientia Marina, 65, 85–105, 2001.

520 Colman, A. S. and Holland, H. D.: The Global Diagenetic Flux of Phosphorus from Marine Sediments to the Oceans: Redox Sensitivity and the Control of Atmospheric Oxygen Levels., in: Marine Authigenesis: From Global to Microbial, vol. 66, p. 53–75, SEPM Society for Sedimentary Geology, https://doi.org/10.2110/pec.00.66.0053, 2000.

Compton, J., Mallinson, D., Glenn, C. R., Filippelli, G., Föllmi, K., Shields, G., and Zanin, Y.: Variations in the global phosphorus cycle, in: Marine Authigenesis: From Global to Microbial, vol. 66, pp. 21–33,, SEPM Society for Sedimentary Geology,

525 https://doi.org/10.2110/pec.00.66.0021, 2000.

Delaney, M. L.: Phosphorus accumulation in marine sediments and the oceanic phosphorus cycle, Global Biogeochemical Cycles, 12 No.4, 563–572, 1998.

Deutsch, C., Gruber, N., Key, R. M., and Sarmiento, J. L.: Denitrification and N_2 fixation in the Pacific Ocean, Global Biogeochemical Cycles, 15, 483–506, 2001.

530   Deutsch, C., Sarmiento, J. L., Sigman, D. M., Gruber, N., and Dunne, J. P.: Spatial coupling of nitrogen inputs and losses in the ocean, Nature, 445, 163–167, 2007.

Dumont, E., Harrison, J. A., Kroeze, C., Bakker, E. J., and Seitzinger, S. P.: Impacts of Atmospheric Anthropogenic Nitrogen on the Open Ocean, Global Biogeochemical Cycles, 19, GB4S02, https://doi.org/10.1029/2005GB002488, 2005.

Eby, M., Zickfeld, K., Montenegro, A., Archer, D., Meissner, K. J., and Weaver, A. J.: Lifetime of Anthropogenic Climate
535   Change: Millennial Time Scales of Potential CO_2 and Surface Temperature Perturbations, Journal of Climate, 22, 2501–2511, https://doi.org/10.1175/2008JCLI2554.1, 2009.

Falkowski, P. G.: Evolution of the nitrogen cycle and its influence on the biological sequestration of CO_2 in the ocean, Nature, 387, 272–275, https://doi.org/10.1038/387272a0, 1997.

Fanning, A. F. and Weaver, A. J.: An atmospheric energy-moisture balance model: Climatology, interpentadal climate change, and coupling
540   to an ocean general circulation model, Journal of Geophysical Research, 101, 15 111–15 128, https://doi.org/10.1029/96JD01017, 1996.

Filipelli, G. M.: The Global Phosphorus Cycle: Past, Present, and Future, Elements, 4, 89–95, https://doi.org/10.2113/GSELEMENTS.4.2.89, 2008.

Flögel, S., Wallmann, K., Poulson, C. J., Zhou, J., Oschlies, A., Voigt, S., and Kuhnt, W.: Simulating the biogeochemical effects of volcanic CO_2 degassing on the oxygen-state of the deep ocean during the Cenomanian/Turonian Anoxic Event (OAE2), Earth Planet Scientific
545   Letters, 305, 371–384, https://doi.org/10.1016/j.epsl.2011.03.0181, 2011.

Föllmi, K. B.: The Phosphorus Cycle, phosphogenesis and marine phosphate-rich deposits, Earth-Science Reviews, 40, 55–124, https://doi.org/10.1016/0012-8252(95)00049-6, 1995.

Galloway, J. N., Dentener, F., Capone, D., Boyer, E., Howarth, R., Seitzinger, S., Asner, G., Cleveland, C., Green, P., Holland, E., Karl, D., Michaels, A., Porter, J., Townsend, A., and Vörösmarty, C.: Nitrogen cycles: past, present, and future, Biogeochemistry, 70, 153–226,
550   https://doi.org/10.1007/s10533-004-0370-0, 2004.

Gao, S., Schwinger, J., Tjiputra, J., Bethke, I., Hartmann, J., Mayorga, E., and Heinze, C.: Riverine impact on future projections of marine primary production and carbon uptake, Biogeochemistry, 20, 93–119, https://doi.org/10.5194/bg-20-93-2023, 2023.

Garcia, H. E., Weathers, K., Paver, C. R., Smolyar, I., Boyer, T. P., Locarnini, R. A., Zweng, M. M., Mishonov, A. V., Baranova, O. K., Seidov, D., and Reagan, J. R.: Volume 3: Dissolved Oxygen, Apparent Oxygen Utilization, and Oxygen Saturation, in: World Ocean Atlas
555   2018, edited by Editor, A. M. T., p. 38pp, NOAA Atlas NESDIS 83, https://www.nodc.noaa.gov/OC5/woa18/pubwoa18.html, 2019a.

Garcia, H. E., Weathers, K., Paver, C. R., Smolyar, I., Boyer, T. P., Locarnini, R. A., Zweng, M. M., Mishonov, A. V., Baranova, O. K., Seidov, D., and Reagan, J. R.: Volume 4: Dissolved Inorganic Nutrients (phosphate, nitrate and nitrate+nitrite, silicate), in: World Ocean Atlas 2018, edited by Editor, A. M. T., p. 35pp, NOAA Atlas NESDIS 84, https://www.ncei.noaa.gov/data/oceans/woa/WOA18/DOC/woa18_vol4.pdf, 2019b.

560   Garnier, J., Beusen, A., Thieu, V., Billen, G., and Bouwman, L.: N:P:Si nutrient export ratios and ecological consequences in coastal seas evaluated by the ICEP approach, Global Biogeochemical Cycles, 24, GB0A05, https://doi.org/10.1029/2009GB003583, 2010.

Giraud, X., Quéré, C. L., and da Cunha, L. C.: Importance of coastal nutrient supply for global ocean biogeochemistry, Global Biogeochemical Cycles, 22, GB2025, https://doi.org/10.1029/2006GB002717, 2008.

Gruber, N.: The Dynamics of the Marine Nitrogen Cycle and its Influence on Atmospheric CO_2 Variations, in: The Ocean Carbon Cycle and
565   Climate, edited by Follows, M. and Oguz, T., pp. 97–148, Springer Netherlands, Dordrecht, https://doi.org/10.1007/978-1-4020-2087-2_4, 2004.

Gruber, N.: The marine nitrogen cycle: Overview and challenges, in: Nitrogen in the Marine Environment, edited by et al., D. G. C., chap. 1, pp. 1–50, Academic Press, San Diego, California, 2 edn., 2008.

Gruber, N. and Sarmiento, J. L.: Global patterns of marine nitrogen fixation and denitrification, Global Biogeochemical Cycles, 11, 235–266, https://doi.org/10.1029/97GB00077, 1997.

Harrison, J. A., Seitzinger, S. P., Bouwman, A. F., Caraco, N. F., Beusen, A. H. W., and Vörösmarty, C. J.: Dissolved inorganic phosphorus export to the coastal zone: Results from a spatially explicit, global model, Global Biogeochemical Cycles, 19, GB4S03, https://doi.org/10.1029/2004GB002357, 2005.

Ingall, E. and Jahnke, R.: Evidence for enhanced phosphorus regeneration from marine sediments overlain by oxygen depleted waters, Geochimica et Cosmochimica Acta, 58, 2571–2575, 1994.

Izett, J. G. and Fennel, K.: Estimating the Cross-Shelf Export of Riverine Materials: Part 1. General Relationships From an Idealized Numerical Model, Global Biogeochemical Cycles, 32, 160–175, https://doi.org/10.1002/ 2017GB005667, 2018.

Johnson, K. S., Riser, S. C., and Ravichandran, M.: Oxygen Variability Controls Denitrification in the Bay of Bengal Oxygen Minimum Zone, Geophysical Research Letters, 46, 804–811, https://doi.org/10.1029/2018GL079881, 2019.

Karl, D., Micheals, A., B.Bergman, Capone, D., Carpenter, E., Letelier, R., Lipschultz, F., Paerl, H., Sigman, D., and Stal, L.: Dinitrogen fixation in the world's oceans, Biogeochemistry, 57/58, 47–98, 2002.

Keller, D. P., Oschlies, A., and Eby, M.: A new marine ecosystem model for the University of Victoria Earth System Climate Model, Geoscientific Model Development, 5, 1195–1220, https://doi.org/10.5194/gmd-5-1195-2012, 2012.

Kemena, T. P., Landolfi, A., Oschlies, A., Wallmann, K., and Dale, A. W.: Ocean phosphorus inventory: large uncertainties in future projections on millennial timescales and their consequences for ocean deoxygenation, Earth System Dynamics, 10, 539–553, https://doi.org/10.5194/esd-10-539-2019, 2019.

Lacroix, F., Ilyina, T., and Hartmann, J.: Oceanic CO_2 outgassing and biological production hotspots induced by pre-industrial river loads of nutrients and carbon in a global modeling approach, Biogesciences, 17, 55–88, https://doi.org/10.5194/bg-17-55-2020, 2020.

Landolfi, A., Dietze, H., Koeve, W., and Oschlies, A.: Overlooked runaway feedback in the marine nitrogen cycle: the vicious cycle, Biogeosciences, 10, 1351–1363, https://doi.org/10.5194/bg-10-1351-2013, 2013.

Landolfi, A., Koeve, W., Dietze, H., Kähler, P., and Oschlies, A.: A new perspective on environmental controls of marine nitrogen fixation, Geophysical Research Letters, 42, 4482–4489, https://doi.org/10.1002/2015GL063756, 2015.

Löscher, C. R., Mohr, W., Bange, H. W., and Canfield, D. E.: No nitrogen fixation in the Bay of Bengal?, Biogeosciences, 17, 851–864, https://doi.org/10.5194/bg-17-851-2020, 2020.

Martiny, A. C., Lomas, M. W., Fu, W., Boyd, P. W., Chen, Y.-I. L., Cutter, G., Ellwood, M. J., Furuya, K., Hashihama, F., Kanda, J., Karl, D. M., Kodama, T., Li, Q. P., Ma, J., Moutin, T., Woodward, E. M. S., and Moore, J. K.: Biogeochemical controls of surface ocean phosphate, Science Advances, 5, eaax0341, https://doi.org/10.1126/sciadv.aax0341, 2019.

Mather, R. L., Reynolds, S. E., Wolff, G. A., Williams, R. G., Torres-Valdes, S., Woodward, E. M. S., Landolfi, A., Pan, X., Sanders, R., and Achterberg, E. P.: Phosphorus cycling in the North and South Atlantic Ocean subtropical gyres, Nature Geoscience, 1, 439–443, https://doi.org/10.1038/ngeo232, 2008.

Mayorga, E., Seitzinger, S. P., Harrison, J. A., Dumont, E., Beusen, A. H. W., Bouwman, A., Fekete, B. M., Kroeze, C., and van Drecht, G.: Global Nutrient Export fromWaterSheds 2 (NEWS 2): Model development and implementation, Environmental Modelling and Software, 25, 837–853, https://doi.org/10.1016/j.envsoft.2010.01.007, 2010.

Mengis, N., Keller, D. P., MacDougall, A. H., Eby, M., Wright, N., Meissner, K. J., Oschlies, A., Schmittner, A., MacIsaac, A. J., Matthews, H. D., and Zickfeld, K.: Evaluation of the University of Victoria Earth System Climate Model version 2.10 (UVic ESCM 2.10), Geoscientific Model Development, 13, 4183–4204, https://doi.org/10.5194/gmd-13-4183-2020, 2020.

Monteiro, F. M., Pancost, R. D., Ridgwell, A., and Donnadieu, Y.: Nutrients as the dominant control on the spread of anoxia and euxinia across the Cenomanian-Turonian oceanic anoxic event (OAE2): Model-data comparison, Paleoceanography, 27, PA4209, https://doi.org/10.1029/2012PA002351, 2012.

Moore, C. M., Mills, M. M., Achterberg, E. P., Geider, R. J., LaRoche, J., Lucas, M. I., McDonagh, E. L., X. Pan, A. J. P., Rijkenberg, M. J. A., Suggett, D. J., Ussher, S. J., and S.Woodward, E. M.: Large-scale distribution of Atlantic nitrogen fixation controlled by iron availability, Nature Geoscience Letters, 2, 867–871, https://doi.org/10.1038/NGEO667, 2009.

Moore, J. K. and Doney, S. C.: Iron availability limits the ocean nitrogen inventory stabilizing feedbacks between marine denitrification and nitrogen fixation, Global Biogeochemical Cycles, 21, GB2001, https://doi.org/10.1029/2006GB002762, 2007.

Nickelsen, L., Keller, D., and Oschlies, A.: A dynamic marine iron cycle module coupled to the University of Victoria Earth System Model: the Kiel Marine Biogeochemical Model 2 (KMBM2) for UVic 2.9, Geoscientific Model Development Discussions, 7, 8505–8563, https://doi.org/10.5194/gmdd-7-8505-2014, 2014.

Niemeyer, D., Kemena, T. P., Meissner, K. J., and Oschlies, A.: A model study of warming-induced phosphorus–oxygenfeedbacks in open-ocean oxygen minimum zones on millennial timescales, Earth System Dynamics, 8, 357–367, https://doi.org/10.5194/esd-8-357-2017, 2017.

Oschlies, A., P.Brandt, Stramma, L., and Schmidtko, S.: Drivers and mechanisms of ocean deoxygenation, Nature Geoscience, 11, 467–473, https://doi.org/10.1038/s41561-018-0152-2, 2018.

Oschlies, A., Koeve, W., Landolfi, A., and Kähler, P.: Loss of fixed nitrogen causes net oxygen gain in a warmer future ocean, Nature Communications, https://doi.org/10.1038/s41467-019-10813-w, 2019.

Palastanga, V., Slomp, C. P., and Heinze, C.: Long-term controls on ocean phosphorus and oxygen in a global biogeochemical model, Global Biogeochemical Cycles, 25, GB3024, https://doi.org/10.1029/2010GB003827, 2011.

Partanen, A.-I., Keller, D. P., Korhonen, H., and Matthews, H. D.: Impacts of sea spray geoengineering on ocean biogeochemistry, Geophyscal Research Letters, 43, 7600–7608, https://doi.org/10.1002/2016GL070111, 2016.

Paulmier, A. and Ruiz-Pino, D.: Oxygen minimum zones (OMZs) in the modern ocean, Global Biogeochemical Cycles, 25, GB3024, https://doi.org/10.1016/j.pocean.2008.08.001, 2009.

Redfield, A. C., Ketchum, B. H., and Richards, F. A.: The Influence of Organisms on the Composition of Sea-Water, in: The Sea Vol. 2, edited by Hill, M. N., pp. 26–27, Interscience, New York, 1963.

Ruttenberg, K. C.: The Global Phosphorus Cycle, in: Treatise on Geochemistry, edited by Schlesinger, W., Elsevier, https://doi.org/https://doi.org/10.1016/B0-08-043751-6/08153-6, 2003.

Santos, I. R., Chen, X., Lecher, A. L., Sawyer, A. H., Moosdorf, N., Rodellas, V., Tamborski, J., Cho, H.-M., Dimova, N., Sugimoto, R., Bonaglia, S., Li, H., Hajati, M.-C., and Li, L.: Submarine groundwater discharge impacts on coastal nutrient biogeochemistry, vol. 2, p. 307–323, https://doi.org/10.1038/s43017-021-00152-0, 2021.

Schmittner, A., Oschlies, A., Giraud, X., Eby, M., and Simmons, H. L.: A global model of the marine ecosystem for long-term simulations: Sensitivity to ocean mixing buoyancy forcing, particle sinking, and dissolved organic matter cycling, Global Biogeochemical Cycles, 19, GB3004, https://doi.org/10.1029/2004GB002283, 2005.

Schmittner, A., Oschlies, A., Matthews, H. D., and Galbraith, E. D.: Future changes in climate, ocean circulation, ecosystems, and bio-geochemical cycling simulated for a business-as-usual CO_2 emission scenario until year 4000 AD, Global Biogeochemical Cycles, 22, GB1013, https://doi.org/10.1029/2007GB002953, 2008.

Seitzinger, S. P., Mayorga, E., Bouwman, A. F., Kroeze, C., Beusen, A. H. W., Billen, G., Drecht, G. V., Dumont, E., Fekete, B. M., Garnier, J., and Harrison, J. A.: Global river nutrient export: A scenario analysis of past and future trends, Global Biogeochemical Cycles, 24, GB0A08, https://doi.org/10.1029/2009GB003587, 2010.

Sharples, J., Middelburg, J. J., Fennel, K., and Jickells, T. D.: What proportion of riverine nutrients reaches the open ocean?, Global Biogeo-chemical Cycles, 31, 39–58, https://doi.org/10.1002/ 2016GB005483, 2017.

Slomp, C. P. and Capellen, P. V.: Nutrient inputs to the coastal ocean through submarine groundwater discharge: controls and potential impact, Journal of Hydrology, 295, 64–86, https://doi.org/10.1016/j.jhydrol.2004.02.018, 2004.

Sohm, J. A., Webb, E. A., and Capone, D. G.: Emerging patterns of marine nitrogen fixation, Nature Reviews Microbiology, 9, 499–508, https://doi.org/10.1038/nrmicro2594, 2011.

Somes, C. J. and Oschlies, A.: On the influence of "non-Redfield" dissolved organic nutrient dynamics on the spatial dis-tribution of N2 fixation and the size of the marine fixed nitrogen inventory, Global Biogeochemical Cycles, 29, 973–993, https://doi.org/10.1002/2014GB005050, 2015.

Somes, C. J., Schmittner, A., Galbraith, E. D., Lehmann, M. F., Altabet, M. A., Montoya, J. P., Letelier, R. M., Mix, A. C., Bourbonnais, A., and Eby, M.: Simulating the global distribution of nitrogen isotopes in the ocean, Global Biogeochemical Cycles, 24, GB4019, https://doi.org/10.1029/2009GB003767, 2010b.

Somes, C. J., Oschlies, A., and Schmittner, A.: Isotopic constraints on the pre-industrial oceanic nitrogen budget, Biogeosciences, 10, 5889–5910, https://doi.org/10.5194/bg-10-5889-2013, 2013.

Somes, C. J., Schmittner, A., Muglia, J., and Oschlies, A.: SA Three-Dimensional Model of theMarine Nitrogen Cycle during the Last Glacial Maximum Constrained by Sedimentary Isotopes, Frontiers in Marine Science, 4:108, https://doi.org/10.3389/fmars.2017.00108, 2017.

Séférian, R., Berthet, S., Yool, A., Palmiéri, J., Bopp, L., Tagliabue, A., Kwiatkowski, L., Aumont, O., Christian, J., Dunne, J., Gehlen, M., Ilyina, T., John, J. G., Li, H., Long, M. C., Luo, J. Y., Nakano, H., Romanou, A., Schwinger, J., Stock, C., Santana-Falcón, Y., Takano, Y., Tjiputra, J., Tsujino, H., Watanabe, M., Wu, T., Wu, F., and Yamamoto, A.: Tracking Improvement in Simulated Marine Biogeochemistry Between CMIP5 and CMIP6, Current Climate Change Reports, 6, 95–119, https://doi.org/10.1007/s40641-020-00160-0, 2020.

Tivig, M., Keller, D. P., and Oschlies, A.: Riverine nitrogen supply to the global ocean and its limited impact on global primary production: a feedback study using an Earth system model, Biogeosciences, 18, 5327–5350, https://doi.org/10.5194/bg-18-5327-2021, 2021.

Tivig, M., Keller, D. P., and Oschlies, A.: UVic simulation with riverine nutrient export from NEWS2 dataset., https://doi.org/hdl:20.500.12085/85adfcd5-bc86-440c-a205-496749a9025f, 2024.

Tyrrell, T.: The relative influences of nitrogen and phosphorus on oceanic primary production, Nature, 400, 525–531, 1999.

Voss, M., Bange, H. W., Dippner, J. W., Middelburg, J. J., Montoya, J. P., and Ward, B.: The marine nitrogen cycle: recent discover-ies, uncertainties and the potential relevance of climate change, Philosophical Transactions of the Royal Society B, 368, 20130121, https://doi.org/10.1098/rstb.2013.0121, 2013.

Wallmann, K.: Phosphorus imbalance in the global ocean?, Global Biogeochemical Cycles, 24, GB4030, https://doi.org/10.1029/2009GB003643, 2010.

Wang, W.-L., Moore, J. K., Martiny, A. C., and Primeau, F. W.: Convergent estimates of marine nitrogen fixation, Nature, 566, 205–211, https://doi.org/10.1038/s41586-019-0911-2, 2019.

680 Weaver, A. J., Eby, M., Wiebe, E. C., Bitz, C., Duffy, P. B., Ewen, T. L., Fanning, A. F., Holland, M. M., MacFadyen, A., Matthews, H. D., Meissner, K. J., Saenko, O., Schmittner, A., Wang, H., and Yoshimori, M.: The UVic Earth System Climate Model: Model Description, Climatology, and Applications to Past, Present and Future Climates, Atmosphere-ocean, 39(4), 361–428, https://doi.org/10.1080/07055900.2001.9649686, 2001.

Zehr, J. P. and Capone, G.: Changing perspectives in marine nitrogen fixation, Science, 368, https://doi.org/10.1126/science.aay9514, 2020.